國立台灣大學 生命科學院 動物學研究所

Institute of Zoology, College of Life Science

National Taiwan University

碩士論文

低溫緊迫下斑馬魚腦內抗氧化機制與解偶聯蛋白相關研究

Exploring uncoupling proteins and anti-oxidative stress mechanisms under acute cold exposure in adult zebrafish brain

陳若冬

Ruo-Dong Chen

指導教授：黃鵬鵬 博士 (Pung-Pung Hwang, Ph.D)

李士傑 博士 (Shyh-Jye Lee, Ph.D)

中華民國 99 年 6 月 June, 2010

謝辭

首先感謝論文口試委員台大動物所嚴震東老師、李士傑老師，海洋大學水產養殖系張清風老師，師範大學生科系林豐益老師給予我的論文和實驗方面的諸多建議與指教；另外，感謝動物所所長陳俊宏老師，在學期中的關心與幫助。

不敢相信，在這一年來經歷媽媽重大車禍的情況下，我還能得以完成論文而畢業。我想我是非常幸運的研究生，從大學到現在，在研究上一直有指引的明燈，就是指導教授黃鵬鵬老師。黃鵬鵬老師對研究的充沛熱情和對實驗的嚴謹態度，總是感染著實驗室的每個人。在家裡發生變故後，感謝黃鵬鵬老師的寬容與信任，讓我能放下手邊的工作，心無旁騖的照顧媽媽。實驗室像是我第二個家，感謝董姐與君琳學姐在很多時候，我的情緒已經到達臨界點時，適時給予建議與開導；感謝怡方、致潔的關心與陪伴；謝謝小峻和大顧總是讓實驗室有著歡樂的氣氛；而大顧的美味蛋糕與食物則是我在實驗室趕工時的最佳能量來源；實驗室的壯丁，阿鼠、老爹與咸台，總是幫我做實驗中最苦力的工作；謝謝王哥在斑馬魚與設備上的諸多幫助；謝謝依純，常常在我分身乏術時，擔任起最佳保母照顧我的小貓；謝謝浩軒在這段時間幫我買晚餐，且擔負了許多雜務工作，讓我得以專心在口試準備上；周銘翊學長在我最初進實驗室時教我 real-time RT-PCR 的方法；謝謝我的朋友 fuzzyspot，即使難得回台，總是抽空稍來最大的問候與關懷；maca 學姊總是以過來人的經驗適時的安慰我。

這篇論文得以完成，最要感謝的是庸哲，不管是實驗架構，邏輯到最後校訂論文的完稿，總是不厭其煩的幫助我，而在生活上大大小小的事物，更是給予無私的協助，沒有他我絕對是無法順利畢業的。

最後，要感謝我最愛的媽媽與姐姐，是媽媽全部的包容與支持，我才得以快樂的做自己想做的事，而一路走到現在。感謝姊姊從小到大的陪伴，不管是遇到多大的困難與悲傷，我們都是互相打氣一起度過；甚至在最後關頭，一肩扛起了照顧媽媽的責任，讓我能無後顧之憂的專心在實驗室完成論文。另外，感謝舅舅與舅媽在這風風雨雨的一年總是提供溫柔與強壯的肩膀，感謝阿姨，表姐妹們的支持給予我積極向前的力量；而小咪總是默默的陪在我身邊，扮演”療癒小物”的角色。特此將這本論文獻給所有我摯愛的家人、師長與朋友。

陳若冬

July, 2010

Contents

中文摘要

對於變溫脊椎動物（包含魚類）而言，環境溫度的改變除了會加速粒線體的呼吸作用，同時也會增加粒線體內活性氧化物（Reactive oxygen species, ROS）的形成。密集的呼吸作用下所產生的過量 ROS 會導致細胞損害。但是藉由粒線體解偶聯蛋白（Uncoupling proteins, UCPs）所引起的緩和性解偶聯作用（Mild uncoupling），與抗氧化酵素的調節，則能夠抑制 ROS 所造成的氧化壓力。然而至今對於魚類腦部處於低溫緊迫下的抗氧化機制仍不清楚。本研究偵測模式動物-斑馬魚在急性寒冷緊迫下（28 °C 轉移至 18 °C），腦內氧化壓力相關指標因子的變化。其中，斑馬魚五個 UCP 亞型（zUCP1, -2, -2l, -4, -5）被清楚註解與確認，並偵測低溫下其 mRNA 在斑馬魚腦內的表現。同時，亦測量在低溫緊迫下，斑馬魚腦部蛋白質羰基(氧化壓力的生物標記)的濃度，和細胞內的抗氧化分子，諸如過氧化氫酵素(Catalase, CAT)的 mRNA 表現量與超氧化歧化酵素(SOD)的活性。實驗結果顯示，除了 *zucp1* 外，其餘四型 *zucps* 皆會受到低溫刺激而有不同的表現趨勢；蛋白質羰基的濃度在低溫刺激下則有顯著增加，另外腦部 SOD 活性與 *cat* 的 mRNA 在低溫緊迫下亦會增加。

另一方面，目前哺乳類研究已知過氧化酶活化增生受體（PPAR）可調控 UCPs 和抗氧化酵素的轉錄。本研究中發現五型的 *zppar* mRNA 在低溫下各有不同的表現趨勢，由此推論低溫緊迫下，神經細胞可能會藉由 PPAR 轉錄調控解偶聯蛋白的基因表現，導致粒線體緩和性解偶聯作用，進而降低 ROS 累積。此外，研究中也發現抗氧化酶與 PPAR 有類似的表現量變化趨勢。另一方面，細胞氧化還原狀態的指標：穀胱甘肽氧化還原率（2GSSG/GSH）和穀胱甘肽含量（Glutathione content），在低溫緊迫下均維持不變。綜合以上推論：斑馬魚腦內除了抗氧化酶的作用外，PPAR-UCP 可能是低溫緊迫下腦部細胞抵抗氧化壓力的另一途徑，同時並參與了代謝平衡的調控與體內平衡的維持。

Abstract

Exposure to fluctuating temperatures accelerates the mitochondrial respiration and increases the formation of mitochondrial reactive oxygen species (ROS) in ectothermic vertebrates including fish. Excess ROS production by intensively respiring mitochondria results in cellular damages, but mild uncoupling mechanism and enzymatically antioxidant adjustments can defense the oxidative stress. However, neuronal defense pathway against oxidative stress in fish brain upon cold stress is unclear so far. In this study, five members of uncoupling proteins (UCPs) of zebrafish (*Danio rerio*) were clearly annotated and identified. Effects of acute cold exposure (from 28 °C to 18 °C) on brains' *zucp* mRNA expressions and oxidative stress parameters were measured. Except the *zucp1*, transcripts of other four *zucps* would be affected by acute 18 °C exposure. Concentrations of cellular protein carbonyl groups (biomarkers of oxidative stress) were significantly increased after cold exposure. Following the cold exposure, anti-oxidative stress parameters, activities of superoxide dismutase (SOD) and transcripts of catalase (CAT), were increased. All the mRNA levels of *zppar* homologs were also found to change after 18 °C exposure. The axis of peroxisome proliferator-activated receptor (PPAR) and UCPs is involved in the defense pathways against ROS. In addition, the similar expression patterns of PPAR and antioxidant enzymes were also found in this study. Furthermore, indicators of the cellular redox situation, glutathione redox ratio and glutathione content, were maintained constant. Taken all together, stimulation of the PPAR-UCP axis results in mitochondrial mild uncoupling, biogenesis activation, and reduction of ROS. Apart from the antioxidant enzymes, this mechanism may be one of the defense pathways for anti-oxidative stress, regulating metabolic balance, and maintaining cellular homeostasis in ectothermic zebrafish brain upon stressful cold exposure.

Introduction

Cold stress in Fish

Temperature is one of the crucial environment factors to ectotherms, especially in aquatic animals. Spatial and temporal fluctuations of temperature in the environments determines all behavioral and physiological responses of animals (Sohal and Allen, 1986). In effect, water temperature has been described as the “abiotic master factor” for fishes (Brett, 1971). Low temperature causes a rapid reduction in body temperature and even associates with the health and survival of fish (Ibarz et al., 2010). Therefore, a physiological cascade of acclimation strategies in fish has been explored to be involved in maintaining cellular homeostasis (Donaldson et al., 2008).

CNS Response to Cold Stress

The vertebrate brain may be the most vulnerable organ to thermal fluctuations, since most of the physiological acclimation responses are initiated by the central nervous system (CNS) (Crawshaw et al., 1985). Van den Burg and collegues found rapid and specific responses in the carp (*Cyprinus carpio*) brain within minutes after the onset of the temperature drop, by using high-resolution functional magnetic resonance imaging (fMRI) (van den Burg et al., 2005; van den Burg et al., 2006). In addition, early studies in green sunfish (*Lepomis cyanellus*) demonstrate that the brain changes in enzyme activities and is highly aerobic during cold exposure (Shaklee et al., 1977). However, the process of aerobic respiration continuously generates reactive oxygen species (ROS) that may escape the mitochondria to cause cellular damage. In addition, during cold exposure, increased polyunsaturation of membrane phospholipids leads to the maintenance of membrane fluidity (Hazel, 1995) and may enhance the oxidative capacity (Abele and Puntarulo, 2004). Taken all together, raising the mitochondrial

respiration rates may lead to some deleterious consequences, including ROS formation, proton leak increment, and lipid peroxidation (Guderley, 2004). Thus, the protective system against ROS production in the CNS during cold induced oxidative stress needs to be studied in fish.

Mitochondrial Oxidative Stress: ROS and Lipid Peroxidation

Mitochondria are located in the cytoplasm of eukaryotic cells and play a crucial rule in cell survival and function, including energy production, calcium homeostasis, and redox regulation (Halliwell and Gutteridge, 2007). Moreover, mitochondria are the metabolic center in cells. During the oxidative phosphorylation, an electrochemical proton gradient (also known as proton motive force) formed by the electron transfer chain (ETC) would drive proton through ATP synthase to produce ATP (Echtay, 2007). In addition to the ATP formation, the mitochondrial is also the major site of cellular ROS generation. During the respiration, at least 2 % of oxygen taken up by mitochondria is transformed into oxygen free radicals or ROS (Balaban et al., 2005). In higher organisms, low levels of ROS function as signaling molecules (Droge, 2002); however, excess ROS is generally the physiological event in intracellular redox signaling cascades, including the initiation of programmed cell death (apoptosis) (Deshmukh and Johnson, 1997).

Oxidative stress occurs when the cellular prooxidant/antioxidant system is in an imbalanced state. Overproduction of ROS by mitochondrial ETC usually results in oxidative stress, which leads to the damage of biomolecules, such as proteins, structural carbohydrates, nucleic acids, and peroxidation of membrane phospholipids (Sies et al., 1985). Among them, peroxidation products are mostly cytocoxic and particularly harmful. Furthermore, lipid peroxidation leads to dispersion of free radical reactions, which may cause further ROS propagation and mitochondrial damage (Mignotte and

Vayssiere, 2001).

Antioxidant System

To defense the oxidative stress and keep the balance of redox state, aerobic cells perform two major antioxidant systems. One mechanism depends on enzymatic adjustments, including activations of superoxide dismutase (SOD), catalase, and peroxidase. In addition, some low molecular weight antioxidants, such as ascorbate, glutathione (GSH), and phenolic compounds, were also involved in antioxidant regulation (Jacob, 1995).

Apart from these two antioxidant groups, it is now known that the protonmotive force has strong positive correlation with ROS production (Hansford et al., 1997; Votyakova and Reynolds, 2001). Therefore, another mechanism, the "mild uncoupling" has been suggested to have a nature antioxidant effect (Brand et al., 2004). Mild uncoupling, i.e. a limited increase in proton conductance of the inner mitochondrial membrane by synthetic uncouplers, decreases both of the components of proton motive force: membrane potential ($\Delta\Psi_m$) and pH gradient, and thus decreases the superoxide production (Echtay et al., 2003).

Uncoupling Proteins (UCPs)

During the mitochondrial respiration, the oxidative phosphorylation is never fully coupled to ATP synthesis *in vivo*, and one reason is the existence of uncoupling proteins (UCPs) (Azzu and Brand, 2010). UCPs belong to the superfamily of mitochondrial anion-carriers (SLC25A) which locate in the mitochondrial inner membrane with a molecular mass of 31-34 kDa and are predicted to have six transmembrane domains. The functional carrier is believed to be formed as a homodimer (Krauss et al., 2005).

UCPs catalyze a proton conductance and dissipate the proton electrochemical gradient that is required for ATP production, which results in the reduction of mitochondrial membrane potential and ROS production (Arsenijevic et al., 2000). The UCPs activity is under delicate control: it is strongly inhibited by purine nucleotides such as ATP and GDP, but it can be also activated by free-fatty acid and superoxide (Cannon et al., 2006). Furthermore, 4-hydroxynoneal, (HNE), a lipid peroxidation product also activate UCPs, may serve as a mediator of mild uncoupling (Echtay et al., 2003).

In mammals, UCPs have five homologues, UCP1-UCP5. The original UCP, UCP1 (SLC25A7, thermogenin) is well known for its role in adaptive non-shivering thermogenesis in brown adipose tissue (BAT). And it presents up to 10 % concentration in the membrane protein (Brand and Esteves, 2005). In addition, UCP2 (SLC25A8) and UCP3 (SLC25A9) have 59 % and 57 % amino-acid identity with UCP1, respectively, and 73 % identity with each other (Krauss et al., 2005). UCP2 is expressed in various tissues including brain, while UCP3 is expressed mainly in heart and skeletal muscles. To date, several models have been postulated to discuss the physiological functions of UCP2 and UCP3 including the modulation of ROS signaling, obesity, and insulin secretion (Brand and Esteves, 2005; Cannon et al., 2006; Mattiasson et al., 2003a). UCP4 (SLC25A27) and UCP5 (SLC25A14, also called BMCP1) have only 30 % sequence similarity to UCP1. They are expressed mainly in the nervous system, however, the studies in UCP4 and UCP5 are insufficient and their physiological roles are still unknown (Azzu and Brand, 2010; Mao et al., 1999).

Peroxisome proliferator-activated receptors (PPARs)

PPARs (Peroxisome proliferator-activated receptors) are ligand-activated transcription factors belonging to the nuclear hormone receptor superfamily. PPARs function as

transcription factors which regulate the expression of different target genes involved in various physiological processes such as energy metabolism and inflammation (Blanquart et al., 2003). PPARs activate the transcription as heterodimers with retinoid X receptors (RXR) by binding to specific response element (PPREs) located in the 5' end region of their target genes (Feige et al., 2006). To date, three PPAR isoforms have been characterized in mammals: PPARα, PPARβ/δ and PPARγ. Each isoform has unique expression pattern, which relates to distinct cellular functions (Bordet et al., 2006).

In recent years, PPARs are identified as pivotal actors in the control of UCPs gene transcription (Villarroya et al., 2007). And, different PPAR isoforms mediate respective UCPs' transcription in their respective tissues (Bugge et al., 2010; Zhang et al., 2007). Among them, PPARα also activates the expression of antioxidant enzymes, including superoxide dismutase (SOD) and glutathione peroxidase (Bordet et al., 2006).

PPAR-UCP axis: Regulation of Oxidative Stress in CNS

Although those UCP studies in early days were focused on thermal production, it is unlikely that most ectothermic animals' UCPs have a role in thermoregulation when facing cold stress. It is because of water behave the high thermal capacity, any metabolic heat generated from mitochondria may lost over the gills instantly (Mark et al., 2006). In addition, cold-induced oxidative stress may play a key role in brain damage (see above), and neuronal UCPs are crucial for reducing the mitochondrial ROS production (Andrews et al., 2005). It is important to elucidate the neuroprotective effects of UCPs and how UCPs are controlled when the CNS is under cold-induced oxidative stress.

The physiological role of PPARs in UCP genes expression and the mechanism of

PPARs in the prevention of oxidative stress and neuroprotection have been reported in several studies (Bordet et al., 2006; Bugge et al., 2010; Villarroya et al., 2007; Zhang et al., 2007). However, recent study suggested that UCPs might play roles for the PPAR transactivation in genome aspect apart from their general function in the mitochondria (Bugge et al., 2010).

Mechanisms of cold-induced brain injury in mammals have been well studied for decades (Chan et al., 2004; Liu et al., 2006a; Zigmond et al., 1974). Although cold challenge in teleost has been broadly studied in many aspects, such as neuroendocrine, osmoregulation and immune responses (Donaldson et al., 2008), relative molecular anti-oxidation information of fishes' CNS on this aspect is deficient. Therefore, the antioxidant mechanisms and PPAR/UCP regulations in teleost when facing cold-induced oxidative stress is worthy to be further researched.

Aims of this study

Zebrafish (*Danio rerio*) is one of the most powerful teleost models for exploring the genetic and developmental biology. Recent studies have showed that zebrafish is also applicable to environmental physiological investigations (Hwang and Lee, 2007; Lin et al., 2008). In addition, the physiological and genetic effects of zebrafish upon cold stress have been demonstrated in several studies (Chou et al., 2008; Tang et al., 1999). The purpose of the present study is using zebrafish as a model animal to elucidate the impacts of the environmental cold stress and the adaptive responses to the cold-induced oxidative stress in ectotherms. The specific aims are as fallows:

(1) Expressions of UCPs and PPARs in zebrafish and their relative responses in brain under environmental low temperature.

(2) The redox state in zebrafish brain under acute cold exposure.

(3) Examination those ROS and oxidative stress relevant parameters in brain during cold acclimation.

(4) The molecular physiological relationship between UCPs and cellular redox signaling pathways in fish brain.

Materials and Methods

Animals

Adult zebrafish (*D. rerio*) brood stocks at the Institute of Cellular and Organismic Biology, Academia Sinica, (Taipei, Taiwan) were kept in local tap water at 28 °C under a 14-h light: 10-h dark photoperiod. Experimental protocols were approved by the Academia Sinica Institutional Animal Care and Utilization Committee (approval no.: RFIZOOHP220782).

Acclimation experiments

Zebrafish acclimated to 28 °C were directly transferred to 18 °C and acclimated for determined time intervals (between 1 h to 24/72 h). Fish were fed during acclimation. At the end of the acclimation period, fish were dissected on ice and organs sampled for total RNA, protein extraction and oxidative stress parameter analysis in liquid nitrogen. Fish were always sacrificed during the same time between 11:00 AM to 1:00 PM in order to normalize the circadian rhythm effects on physiological metabolism.

Preparation of mRNA

The total RNA was extracted by homogenizing zebrafish tissues (brain, gill, muscle, skin, heart, liver, spleen, intestine, kidney, eye, and fin) in Trizol Reagent (Invitrogen, Carlsbad, CA, USA) and DNA contamination removed with DNase I (Promega, Madison, WI, USA). The mRNA for the RT-PCR was obtained with a QuickPrep Micro mRNA Purification Kit (Amersham Pharmacia, Piscataway, NJ, USA) according to the supplier protocol. The amount of mRNA was determined by spectrophotometry (ND-1000, NanoDrop Technol, Wilmington, DE), and the mRNA quality was checked by running electrophoresis in RNA denatured gels. All mRNA pellets were stored at -20

°C.

Phylogenetic and genomic analysis

The full-length coding sequences of known zebrafish UCP homologs were retrieved from the GenBank. To verify the membership of identified candidates in the core UCP proteins, the deduced amino acid sequences of zebrafish UCPs were aligned with ClustalX together with all known UCP protein sequences available in public databases and subjected to phylogenetic inferences using the Neighbor-joining (NJ) method. One thousand bootstrap replicate analyses were carried out with Mega4.0. Physical gene maps of verified *ucp* loci were scaled based on assemblies of the Ensembl Genome Browser. Genes located up- and downstream of *ucp* genes in these loci were blasted against mammalian genomes to determine the highest score.

The zebrafish UCPs, PPARs and catalase sequences obtained from GenBank were used to design PCR primers for real-time reverse transcriptase PCR and to generate probes for *in situ* hybridization; theses various primers are summarized in Table 1.

Brain sections *in situ* hybridization

Fresh zebrafish brains were fixed with 4 % paraformaldehyde at 4 °C for 3h, and then gradually immersed in PBS containing different concentrations of sucrose of 5 %, 10 %, and 20 % at 4 °C. Samples were soaked in a mixed PBS solution (OCT compound: 20 % sucrose 1: 2) overnight, and were then embedded with OCT compound-embedding medium (Sakura, Tokyo, Japan) at -20 °C. Cryosections at 10 μm were made with a cryostat (CM 1900, Leica, Heidelberg, Germany), and were applied to poly-L-lysine-coated slides (Erie, Hooksett, NH, USA).

For *in situ* hybridization, digoxigenin (DIG)-labeled (Perkin-Elmer, Boston, MA,

USA) RNA probes were synthesized by *in vitro* transcription with SP6 RNA polymerase (Takara, Shiga, Japan). Brain *in situ* hybridization was performed as previously described (Thisse et al., 2004) and conducted with the nitro blue tetrazolium (NBT) and 5-bromo-4-chloro-3-indolyl phosphate (BCIP) system.

Real-time quantitative (q)PCR

Total RNA was extracted and reverse-transcribed from adult brains of zebrafish as described above. The mRNA expressions of target genes were measured by qPCR with the Roche LightCycler® 480 System (Roche Applied Science, Mannheim, Germany). Primers for all genes were designed (Table 1) using Primer Express software (vers. 2.0, Applied Biosystems). PCRs contained 40 ng of cDNA, 50 nM of each primer, and the LightCycler® 480 SYBR Green I Master (Roche) in a final volume of 10 µl. All qPCR reactions were performed as follows: 1 cycle of 50 °C for 2 min and 95 °C for 10 min, followed by 45 cycles of 95 °C for 15 sec and 60 °C for 1 min (the standard annealing temperature of all primers). PCR products were subjected to a melting-curve analysis, and representative samples were electrophoresed to verify that only a single product was present. Control reactions were conducted with sterile water to determine levels of the background and genomic DNA contamination. The standard curve of each gene was confirmed to be in a linear range with ribosomal protein L13a (RPL13A) as an internal control.

Protein carbonyl contents measurement

Carbonyl groups were measured as indication for oxidative damage of proteins. In order to avoid high concentration of nucleic acid in tissue erroneously contribute to higher estimation of carbonyl contents, the brain homogenates were incubated in a final

concentration of 1 % streptomycin sulfate for 30 min at room temperature and removed the nucleic acid precipitates by centrifuging at 6000 g for 10 min at 4 °C. Brain protein carbonyls were measured using OxiSelect Protein Carbonyl ELISA kit (Cell Biolabs, San Diego, CA, USA) following the manufacturer´s protocol. The contents of protein carbonyl were measured at 450 nm in a Synergy HT spectrophotometer (BIO-TEK, Winooski, Vermont, USA). All samples were analyzed in three parallel measurements at least.

Determination of superoxide dismutase (SOD) activity

Superoxide dismutase (SOD; E.C: 1.15.1.1) activity was determined by a xanthine/xanthine oxidase (XOD) and NBT-based assay system which generates $O_2\bullet^-$ that interacts with NBT to produce and a water-soluble formazan dye (OxiSelect SOD assay kit, Cell Biolabs). Sample absorbance was read at 490 nm in a Synergy HT spectrophotometer microplate reader (BIO-TEK, Winooski, Vermont, USA). All samples were analyzed in three parallel measurements at least.

Determination of reduced (GSH) and oxidized (GSSG) glutathione in brain

The content of GSH and GSSG was analyzed in a glutathione cycling assay according to Heise et al. (2007). Furthermore, the GSSG is formed by oxidation of two GSH molecules; total glutathione content was calculated as the sum (2 GSSG + GSH). Accordingly, the redox ratio of oxidized to reduced glutathione was expressed as 2 GSSG/GSH.

Statistical analysis

Values are presented as the mean ± standard deviation (SD) and compared using

Student's *t*-test or one-way analysis of variance (ANOVA) (with Tukey's pairwise comparison).

Results

Phylogenetic analysis, sequence identity and gene structures of zUCPs

Multiple sequence alignment and phylogenetic (NJ) analysis with homologs of other species clearly identified 5 members of the zUCP family which enable identification of these homologs relationship unambiguously (Fig. 1). The relative sequence identity between zUCPs is shown in Table 2. To further identify these *zucp* genes, comprehensive searches were performed to confirm these orthologs and compare their genomic locations, based on their genome sequence databases (Fig. 2-5). In the genome sequences of zebrafish, each isoform of *zucps* was located at a respective chromosome except *zucp2* and *zucp2l*, which were located between 34.13 mega base-pairs (Mb) and 34.21 Mb in the same chromosome 10 (Fig. 3). Further, gene arrangements in the genomic regions encompassing *ucps* were compared. As shown in Fig. 2-5, *zucp* genes have their own respective syntenies. Comparing the gene arrangements between each *zucp* isoform with its mammalian counterpart (Fig. 2-5), conserved synteny of *ucp1* was found across humans, rodents, amphibians and fish (Fig. 2). In the genome sequences of humans and rodents, *ucp2* and *ucp3* are located next to each other, whereas chicken and amphibians had only *ucp3* and *ucp2*, respectively (Fig. 3). Exact phylogenetic analysis, revealed *ucp2-like* (*ucp2l*) genes are newly assembled in zebrafish, tetradon (*Tetraodon nigroviridis*) and pufferfish (*Fugu rubripes*) (Fig. 3). In addition, gene arrangements of *ucp2* and *ucp2l* in the genomic regions encompassing the new isoforms were also compared. These novel homologs in zebrafish, tetradon and pufferfish were located adjacent to *ucp2* on the same chromosome (Fig. 3). Phylogenetic inference apparently grouped SLC25A27 (UCP4) and SLC25A14 (UCP5) into another root from other members (Fig. 1). The conserved syntenies found around *ucp4* and *ucp5* between humans and rodents were not simultaneously observed in chromosomes of chicken,

amphibians and fish (Fig. 4, 5).

zucp mRNA expressions in zebrafish at 28 °C

Expressions of *zucp* mRNAs were evaluated by RT-PCR in different zebrafish tissues (Fig. 6). All isoforms were expressed in brain, heart, spleen, intestine and kidney. mRNA expressions of the *zucp2* and *zucp5* isoforms were ubiquitously expressed in all tissues. Contrary, mRNA levels of *zucp4* were low compared to other paralogs in all tissues.

Localization of _zucp_ mRNAs in zebrafish brain at 28 °C

In subsequent experiments, specific RNA probes were designed to conduct *in situ* hybridization of the 5 *zucp* isoforms in zebrafish brain cryo-sections. Fig. 7K shows dorsal view of the adult zebrafish brain. As shown in Fig. 7A and F, *zucp1* was confirmed to be predominately localized in the anterior part of the medial division of the cerebellar crest (CC), the valvula crebelli (Vam), the periventricular gray zone of the optic tectum (PGZ) and the ventromedial thalamic nucleus (VM). mRNA of *zucp2* was strongly stained in CC, caudal lobe of the cerebellum (LCa), the cerebellar corpus (CCe), the dorsal posterior thalamic nucleus (DP), the granular eminence (EG), the habenula (Ha), the lateral nucleus of the ventral telecephalic area (Vl), the longitudinal torus (TL), the lateral division of the valvula cerebelli (Val), PGZ and VM (Fig. 7B and G). Positive signals for *zucp2l* were observed in the central posterior thalamic nucleus (CP), CC, PGZ, Vam and VM (Fig. 7C and H). Further, expressions of *zucp4* in zebrafish brains were found in CC, CCe, EG, LCa, PGZ, periventricular nucleus of posterior tuberculum (TPp), Val and VM (Fig. 7D and I). Furthermore, *zucp5* was localized in brain areas of CCe, EG, LCa, PGZ and VM (Fig. 7E and J). These results

indicate all *zucp* homologs to be expressed in PGZ and VM regions.

Effects of cold acclimation on mRNA expression patterns of *zucps* in zebrafish brain

The time-course changes of *zucp*s' mRNA expression levels in zebrafish brain transferring from 28 °C to 18 °C between 1 h to 24 h are shown in Fig. 8, with *zrpl13a* as a house keeping gene. At 28 °C control temperature, *zucp1* and *zucp5* were stronger expressed in brains compared to *zucp2l* and *zucp4* (Fig. 8). Furthermore, *zucp5* exhibited the highest mRNA levels in zebrafish brains and was about 80-fold higher expressed than *zucp4* at 28 °C living circumstances. During cold-shock and a 6 h cold acclimation period, *zucp1* transcript expression remained stable, whereas expression of *zucp2* increased significantly by about 3-fold compared to brains of control fish. This high induction level was maintained up to 24 h post-transfer. In addition, the *zucp2l* mRNA expression was significantly induced after 24 h at 18 °C. Expression of *zucp4* transcript in brain was generally very low, but was immediately up-regulated within 1 h of acute cold shock but returned to where after expression returned to control level after 6 h at 18 °C. Further, at 24 h of 18 °C cold exposure, *zucp4* transcript levels were below control level. The time profile of brain *zucp5* mRNA expression during cold exposure resembles that of *zucp2l*, but this transcript was statistically up-regulated 1 h after transfer to 18 °C where after the expression declined again at 6 h below control level (28 °C) and recovered control levels and 1 h levels at until 24 h exposure. These results in zebrafish brain demonstrate that mRNA expressions of 4 *zucp* isoforms are significantly affected by cold stress, except the *zucp1*.

Time-course of changes of oxidative stress parameters in zebrafish brain

Protein Carbonyl groups

Protein is a major target of oxygen free radicals and other reactive species during several organismic stresses. Fig. 9 presented the time-course of protein carbonyls concentrations in zebrafish brain at different time points after transfer from 28 °C to 18 °C. Protein carbonyl content increased significantly by about 38 % (p<0.05) within the 1st hour of acute cold shock, where after concentrations declined dramatically to very low levels at 6 h of cold exposure. After 6 h, brain carbonyl content increased again to significantly above control level at 24 h and 72 h of cold acclimation.

SOD activities

The time pattern of SOD activity during cold exposure (Fig. 10) can be related to the protein carbonyl values over time (Fig. 9). SOD activity remained constant compared to the non-transfer group within the 1st hour after transfer to 18 °C and then increased dramatic (of about 1.6-fold) at 6 h cold exposure. On prolonged exposure to 18 °C, SOD activity decreased again to control level.

Catalase mRNA expressions

Zebrafish catalase (*zcat*) transcript expression in brain increased rapidly during the 1st h of cold exposure (of about 1.9-fold, Fig. 11), whereas expression levels at 6 h cold exposure were back to control level. At the 24th h following cold transfer, *zcat* mRNA expression increased again to values above the 6th h expression level.

Determination of glutathione state in brains of zebrafish

Neither the ratio of oxidized (GSSG) to reduced (GSH) glutathione, nor the total glutathione content in zebrafish brain changed significantly between controls and the cold exposed group at any time point (Fig. 12A, B), indicating that brain redox state is maintained constant in zebrafish exposed to acute cold stress.

mRNA expression of peroxisome proliferators-activated receptors (PPARs)

Zebrafish carry five *ppar* homologs and all of them are expressed in brain (Fig. 13A-E). Upon exposure to cold stress, *zpparαa* transcript levels in brain were significantly decreased at the 6th h after transfer (Fig. 13A). mRNA levels of *zpparαb* were up-regulated at the 1st and 24th h in the cold, whereas at 6 h post-transfer transcription was control level (Fig. 13B). The mRNA expression of *zpparδa* was greatly up-regulated at the 6 h and then decreased slightly to levels still above controls at 24 h in the cold (Fig. 13C). Across all 5 PPAR isoforms in zebrafish brain, *zpparδb* and *zpparγ* had the highest and lowest mRNA expression, respectively (Fig. 13D, E). The profile of *zpparδb* and *zpparγ* mRNA expression in cold exposed fish were similar to that of *zpparαb* (Fig. 13B, D, E), exhibiting a gradual increase over the time of cold exposure.

Discussion

The major findings of the current studies are as follows. Among all species, it is the 1st time to clearly annotate all members of UCPs, five paralogs, in one species (zebrafish) within an integral study. Based on the phylogenetic analysis, *zucp2* has two paralogs in chromosome 10. Moreover, all the *zucp* isoforms expressed at the respective regions of the brain, and only the *zucp1* mRNA expression was not affected by ambient low (18 °C) temperature. In addition, cellular oxidative stress biomarkers, contents of protein carbonyl groups, increased dramatically upon 18 °C in brain (with a exceptional decrement occurred at the 6th hour after exposure). Simultaneously, anti-oxidative stress parameters, SOD and CAT, were also increased after 1 h 18 °C transfer. After checking the cellular redox situation in brains, the glutathione redox ratio and glutathione content were both maintained constant during 18 °C treatment. Patterns of *zppar* homologs' mRNA expressions implied that stimulation of the PPAR-UCP axis results in the increments of cellular mitochondrial thermogenesis and biogenesis.

Concerning the evolution issue about UCPs, an invertebrate study on UCP homologs (Sokolova and Sokolov, 2005) proposed that the divergence of UCPs is an early evolutionary event, which corresponds to the functional diversity of this protein family. In the present study, the diverse expressions of zUCP1-5 according to their tissue distribution and physiological conditions were observed, supporting the hypothesis proposed by (Sokolova and Sokolov, 2005). In addition, Saito and colleagues proposed that the non-shivering thermogenesis function of mammalian UCP1 may be due to the acquisition of function by positive Darwinian selection. And, vertebrate UCP1-3 acquired much of their diversity through two rounds of gene duplication. The vertebrate proto-UCP first duplicated into UCP1 and ancestral UCP2/UCP3, and then the second gene duplication produced the UCP2 and UCP3 (Saito et al., 2008). As

shown in Fig. 3, duplication of UCP2 (*ucp2* and *ucp2l*) was observed in teleost fishes. The duplication occurred in the same chromosome of fishes similar to the loci appearances of UCP2 and UCP3 in the mammalian counterparts. However, the amino-acid identity between *zucp2* and *zucp1* (72 %) was higher than that between *zucp2* and *zucp2l* (50 %) (Table 2). Moreover, *zucp2l* also showed different expression pattern comparing to human *ucp3* (Vidal-Puig et al., 1997). Taken all together, the results imply that there might be a great dissimilarity in the UCPs' physiological functions between fish and mammals. Thus, independent experiments of each UCP gene in teleosts are needed for further characterizing these paralogs precisely.

In mammals, since the first uncoupling protein (UCP1) in BAT was discovered (Nicholls et al., 1978), the various roles of UCP paralogs have been widely discussed. For ectothermic vertebrates, several UCP paralogs were cloned from fish, including common carp (*C. carpio*) (Jastroch et al., 2005a; Stuart et al., 1999), common eelpouts (*Zoarces viviparous*) (Mark et al., 2006), gilthead sea bream (*Sparus aurata* L.) (Bermejo-Nogales et al., 2010), pufferfish (Jastroch et al., 2005b), rainbow trout (*Oncorhynchus mykiss*) (Coulibaly et al., 2006), red sea bream (*Pagrus major*) (Liang et al., 2003), and zebrafish (Stuart et al., 1999). For fish, they have to cope with the wide fluctuations of ambient temperature in their habitats, and their metabolic rates change following the environmental temperature. Therefore, efficient metabolism in mitochondria for moderating energy demand according to variant temperature is essential for fish (Mark et al., 2006; Portner et al., 2005). Due to their energy dissipating potential, UCP homologs in ectotherms might thus involve in other biological processes that are associated with thermal adaptation. In the previous investigations in fish, the mRNA and/or protein expressions of UCP1, -2, and -3 in liver, muscle, and brain were affected upon temperature fluctuations (Bermejo-Nogales et al., 2010; Jastroch et al.,

2007b; Mark et al., 2006). Although the brain is the organ that senses temperature and makes instruction to cold acclimation (Donaldson et al., 2008), an integral study discuss all UCP isoforms in fish brain during cold stress is still absent to date.

According to the results of RT-PCR (Fig. 5) and *in situ* hybridization (Fig. 7), all the five *zucp* isoforms were expressed in zebrafish brain with respectively specific distributions. In addition, all five *zucp* isoforms were detected in the PGZ of optic tectum, thalamus, and cerecellum (Table 3). Simultaneously, similar distribution pattern in PGZ of optic tectum between zUCPs and carp UCP1 (Jastroch et al., 2007a) infers that these orthologs in the brain of fish may be related to the control of sensory functions. Taken all together, the UCP homologs' distribution patterns in brain suggest that they may participate in neuronal circuitries and behavioral thermoregulation, motor functions and metabolic homeostasis (Amo et al., 2010; Friedlander et al., 1976; Jastroch et al., 2007a; Prosser and Nelson, 1981; Wullimann, 1997).

In mammals, the overproduction of ROS has been observed in many experimental models of CNS injury and neurodegenerative diseases (Andrews et al., 2005). Fishes acclimated to low temperature often possess deleterious ROS accumulation (Guderley, 2004). Since mitochondria is considered as one of the main sources for intracellular ROS, UCPs could be important modifiers of CNS damage by regulating mitochondrial ROS levels (Kim-Han and Dugan, 2005; Mattiasson et al., 2003b). In zebrafish, except the *zucp1*, the other 4 *zucps* in the brain behaved respective expressions upon acute cold exposure (Fig.9), suggesting the divergent roles of the 4 *zucp* isoforms in metabolic balance in fish brain. In addition, this result also infers that the zUCPs may participate in modulating the mitochondrial ROS levels, thus protect the brain from the oxidative damage. The previous study in endotherms' brain cells denoted that the induction of UCP4 may mediate an adaptive shift of energy metabolism for neuroprotective

mechanisms. Increment of glucose uptake and glycolysis for reduced mitochondrial ATP production from oxidative phosphorylation is crucial for attenuating cellular oxidative stress (Liu et al., 2006b). These series of observations have opened a new window for fish physiology concerning the UCP activations, ROS regulation, and relevant metabolic balance in brain's homeostasis. Moreover, it is another interesting issue to study whether the anaerobic glycolysis or vasoconstriction upon stressful cold exposure is beneficial for fish brain.

In brains of zebrafish, SOD and catalase, the antioxidant enzymes against cold-induced oxidative stress were both induced at different time points after transfer from 28 °C to 18 °C (Fig. 10, 11). In addition, the GSSG to GSH ratio and total glutathione content remained unchanged, which can be interpreted as the tissue's redox environment and mitochondrial metabolic balance maintained at stable situation. Upon acute 18 °C exposure, the appearance and swimming ability of zebrafish remained regularly, and the ambient temperature suddenly changes did not cause mortality (data not shown). Therefore, the above antioxidant mechanisms may build up a well complementary system to properly control the mitochondrial respiration. Consequently, ectothermic fish may rely on this physiological ability to cope with the acute oxidative stress. However, whether the cellular protection mechanism against ROS in ectothermic fish is a temporary reaction or a sustained motivation is an interesting issue and remains further investigations.

The transcriptional activation of PPAR-induced neuroprotection including oxidative stress modulation and anti-inflammatory effect has been postulated in recent studies (Bordet et al., 2006). In brains of zebrafish, the various mRNA expression patterns of diverse types/isoforms PPAR represent different responses after cold exposure (Fig. 13). In addition, the mRNA expression patterns of *zucp2* and

zucp2l/zucp5 were similar to that of *zpparγ* and *zpparδb,* respectively (Fig. 8, 13D, E), which implies that different *zppar* homologs may induce the expression of respective *zucps*. Apart from the control of UCPs gene expression, to date, emerging evidences have denoted that mammals' PPARs may participate in the modulating transcriptional expression of antioxidant enzymes, including SOD and catalase (Girnun et al., 2002; Li et al., 2008; Toyama et al., 2004). SOD1 was reported to be activated partly through the PPRE in its promoter (Yoo et al., 1999). In the study of PPARδ knockout in adult mouse heart, PPARδ was proved to regulate both SOD1 and SOD2 expression (Wang et al., 2010). In the present study, the expression pattern of brains' SOD activity was parallel to that of *zpparδa*; both of them showed a dramatic increase and decrease at the 6 th and 24th hour post-transfer, respectively (Fig. 10, 13C). Furthermore, the PPRE has been recently identified in the promoter area for the catalase gene (Girnun et al., 2002). And, catalase has been proposed as one of the target enzymes of PPARα in rat liver (Toyama et al., 2004). In brains of zebrafish, *zcat* and *zpparαb* mRNA expressions also showed parallel pattern; which was upregulated at the 1st and 24th hour (Fig. 11, 13B).

In the present study, it is the first time to indicate that PPAR activation pathways may regulate the expressions of anti-oxidative enzymes and UCPs in ectothermic fish under acute temperature changes. Fig. 14 summarizes the physiological mechanisms that are postulated in the present study. Cold exposure increases ROS production in the brains of zebrafish. Catalase is a major pathway for the reduction of intracellular H_2O_2 produced by SOD. And increased PPAR expressions enhance the activity of antioxidant enzymes, including SOD and catalase, thus decrease the superoxide accumulation. PPAR also activate the expression of UCPs, therefore, the mitochondrial ROS levels are reduced by mild uncoupling mediated by UCPs. These integrated studies in ectotherms not only provide novel insights into an antioxidant mechanism through PPAR pathways,

but also a mitochondrial metabolic adjustment via UCP activation in brains under cold disturbance. The rapid physiological adaptation may enable fish to cope with rigorous temperature drops without incurring death at once.

References

Abele, D., and Puntarulo, S. (2004). Formation of reactive species and induction of antioxidant defence systems in polar and temperate marine invertebrates and fish. Comp Biochem and Physiol A Mol Integr Physiol *138*, 405-415.

Amo, R., Aizawa, H., Takahoko, M., Kobayashi, M., Takahashi, R., Aoki, T., and Okamoto, H. (2010). Identification of the Zebrafish Ventral Habenula As a Homolog of the Mammalian Lateral Habenula. J Neurosci *30*, 1566-1574.

Andrews, Z.B., Diano, S., and Horvath, T.L. (2005). Mitochondrial uncoupling proteins in the CNS: in support of function and survival. Nat Rev Neurosci *6*, 829-840.

Arsenijevic, D., Onuma, H., Pecqueur, C., Raimbault, S., Manning, B., Miroux, B., Couplan, E., Alves-Guerra, M., Goubern, M., and Surwit, R. (2000). Disruption of the uncoupling protein-2 gene in mice reveals a role in immunity and reactive oxygen species production. Nat genet *26*, 435-439.

Azzu, V., and Brand, M.D. (2010). The on-off switches of the mitochondrial uncoupling proteins. Trends Biochem Sci *35*, 298-307

Balaban, R., Nemoto, S., and Finkel, T. (2005). Mitochondria, oxidants, and aging. Cell *120*, 483-495.

Bermejo-Nogales, A., Calduch-Giner, J.A., and Perez-Sanchez, J. (2010). Gene expression survey of mitochondrial uncoupling proteins (UCP1/UCP3) in gilthead sea bream (*Sparus aurata* L.). J Comp Physiol B *180*, 685-694.

Blanquart, C., Barbier, O., Fruchart, J.C., Staels, B., and Glineur, C. (2003). Peroxisome proliferator-activated receptors: regulation of transcriptional activities and roles in inflammation. J Steroid Biochem Mol Biol *85*, 267-273.

Bordet, R., Ouk, T., Petrault, O., Gele, P., Gautier, S., Laprais, M., Deplanque, D., Duriez, P., Staels, B., and Fruchart, J. (2006). PPAR: a new pharmacological target

for neuroprotection in stroke and neurodegenerative diseases. Biochem Soc Trans *34*, 1341-1346.

Brand, M., Affourtit, C., Esteves, T., Green, K., Lambert, A., Miwa, S., Pakay, J., and Parker, N. (2004). Mitochondrial superoxide: production, biological effects, and activation of uncoupling proteins. Free Radic Biol Med *37*, 755-767.

Brand, M.D., and Esteves, T.C. (2005). Physiological functions of the mitochondrial uncoupling proteins UCP2 and UCP3. Cell Metab *2*, 85-93.

Brett, J. (1971). Energetic responses of salmon to temperature. A study of some thermal relations in the physiology and freshwater ecology of sockeye salmon (*Oncorhynchus nerkd*). Integr Comp Biol *11*, 99.

Bugge, A., Siersbaek, M., Madsen, M.S., Göndör, A., Rougier, C., and Mandrup, S. (2010). A novel intronic peroxisome proliferator activated receptor (PPAR) γ enhancer in the uncoupling protein (UCP) 3 gene as a regulator of both UCP2 and -3 expression in adipocytes. J Biol Chem *285*, 17310.

Cannon, B., Shabalina, I.G., Kramarova, T.V., Petrovic, N., and Nedergaard, J. (2006). Uncoupling proteins: A role in protection against reactive oxygen species--or not? Biochim Biophys Acta *1757*, 449-458.

Chan, P., Yang, G., Chen, S., Carlson, E., and Epstein, C. (2004). Cold-induced brain edema and infarction are reduced in transgenic mice overexpressing CuZn-superoxide dismutase. Ann Neurol *29*, 482-486.

Chou, M., Hsiao, C., Chen, S., and Chen, I. (2008). Effects of hypothermia on gene expression in zebrafish gills: upregulation in differentiation and function of ionocytes as compensatory responses. J Exp Biol *211*, 3077.

Coulibaly, I., Gahr, S.A., Palti, Y., Yao, J., and Rexroad, C.E., 3rd (2006). Genomic structure and expression of uncoupling protein 2 genes in rainbow trout

(*Oncorhynchus mykiss*). BMC genomics *7*, 203.

Crawshaw, L., Grahn, D., Wollmuth, L., and Simpson, L. (1985). Central nervous regulation of body temperature in vertebrates: Comparative aspects. Pharmacol Ther *30*, 19-30.

Deshmukh, M., and Johnson, E. (1997). Programmed cell death in neurons: focus on the pathway of nerve growth factor deprivation-induced death of sympathetic neurons. Mol Pharmacol *51*, 897.

Donaldson, M., Cooke, S., Patterson, D., and Macdonald, J. (2008). Cold shock and fish. J Fish Biol *73*, 1491-1530.

Droge, W. (2002). Free radicals in the physiological control of cell function. Physiol Rev *82*, 47.

Echtay, K. (2007). Mitochondrial uncoupling proteins--what is their physiological role? Free Radic Biol Med *43*, 1351-1371.

Echtay, K., Esteves, T., Pakay, J., Jekabsons, M., Lambert, A., Portero-Otin, M., Pamplona, R., Vidal-Puig, A., Wang, S., and Roebuck, S. (2003). A signalling role for 4-hydroxy-2-nonenal in regulation of mitochondrial uncoupling. EMBO J *22*, 4103.

Feige, J.N., Gelman, L., Michalik, L., Desvergne, B., and Wahli, W. (2006). From molecular action to physiological outputs: Peroxisome proliferator-activated receptors are nuclear receptors at the crossroads of key cellular functions. Prog Lipid Res *45*, 120-159.

Friedlander, M., Kotchabhakdi, N., and Prosser, C. (1976). Effects of cold and heat on behavior and cerebellar function in goldfish. J Comp Physiol A Neuroethol Sens Neural Behav Physiol *112*, 19-45.

Girnun, G.D., Domann, F.E., Moore, S.A., and Robbins, M.E.C. (2002). Identification

of a Functional Peroxisome Proliferator-Activated Receptor Response Element in the Rat Catalase Promoter. Mol Endocrinol *16*, 2793-2801.

Guderley, H. (2004). Metabolic responses to low temperature in fish muscle. Biol Rev Camb Philos Soc *79*, 409-427.

Halliwell, B., and Gutteridge, J. (2007). Free radicals in biology and medicine (Oxford University Press Oxford).

Hansford, R., Hogue, B., and Mildaziene, V. (1997). Dependence of H_2O_2 formation by rat heart mitochondria on substrate availability and donor age. J Bioenerg Biomembr *29*, 89-95.

Hazel, J.R. (1995). Thermal adaptation in biological membranes: is homeoviscous adaptation the explanation? Annu Rev Physiol *57*, 19-42.

Heise, K., Estevez, M., Puntarulo, S., Galleano, M., Nikinmaa, M., Portner, H., and Abele, D. (2007). Effects of seasonal and latitudinal cold on oxidative stress parameters and activation of hypoxia inducible factor (HIF-1) in zoarcid fish. J Comp Physiol B *177*, 765-777.

Hwang, P.-P., and Lee, T.-H. (2007). New insights into fish ion regulation and mitochondrion-rich cells. Comp Biochem Physiol A Mol Integr Physiol *148*, 479-497.

Ibarz, A., Padros, F., Gallardo, M., Fernandez-Borras, J., Blasco, J., and Tort, L. (2010). Low-temperature challenges to gilthead sea bream culture: review of cold-induced alterations and "Winter Syndrome". Rev Fish Biol Fisheries, 1-18.

Jacob, R. (1995). The integrated antioxidant system. Nutrition Research *15*, 755-766.

Jastroch, M., Buckingham, J., Helwig, M., Klingenspor, M., and Brand, M. (2007a). Functional characterisation of UCP1 in the common carp: uncoupling activity in liver mitochondria and cold-induced expression in the brain. J Comp Physiol B

177, 743-752.

Jastroch, M., Buckingham, J.A., Helwig, M., Klingenspor, M., and Brand, M.D. (2007b). Functional characterisation of UCP1 in the common carp: uncoupling activity in liver mitochondria and cold-induced expression in the brain. J Comp Physiol B *177*, 743-752.

Jastroch, M., Wuertz, S., Kloas, W., and Klingenspor, M. (2005a). Uncoupling protein 1 in fish uncovers an ancient evolutionary history of mammalian nonshivering thermogenesis. Physiol Genomics *22*, 150-156.

Jastroch, M., Wuertz, S., Kloas, W., and Klingenspor, M. (2005b). Uncoupling protein 1 in fish uncovers an ancient evolutionary history of mammalian nonshivering thermogenesis. Physiol Genomics *22*, 150.

Kim-Han, J.S., and Dugan, L.L. (2005). Mitochondrial uncoupling proteins in the central nervous system. Antioxid Redox Signal *7*, 1173-1181.

Krauss, S., Zhang, C.-Y., and Lowell, B.B. (2005). The mitochondrial uncoupling-protein homologues. Nat Rev Mol Cell Biol *6*, 248-261.

Li, J., Patel, V., Kostetskii, I., Xiong, Y., Chu, A., Jason, T., Yu, C., Morley, G., Molkentin, J., and Radice, G. (2008). Cardiac-specific loss of N-cadherin leads to alterations in connexins with conduction slowing and arrhythmogenesis. Circulation Research. Am Heart Assoc *2008*, 08-14.

Liang, X.F., Ogata, H.Y., Oku, H., Chen, J., and Hwang, F. (2003). Abundant and constant expression of uncoupling protein 2 in the liver of red sea bream Pagrus major. Comp Biochem Physiol A Mol Integr Physiol *136*, 655-661.

Lin, T.Y., Liao, B.K., Horng, J.L., Yan, J.J., Hsiao, C.D., and Hwang, P.P. (2008). Carbonic anhydrase 2-like a and 15a are involved in acid-base regulation and Na^+ uptake in zebrafish H^+-ATPase-rich cells. Am J Physiol Cell Physiol *294*,

C1250-1260.

Liu, D., Chan, S., de Souza-Pinto, N., Slevin, J., Wersto, R., Zhan, M., Mustafa, K., de Cabo, R., and Mattson, M. (2006a). Mitochondrial UCP4 mediates an adaptive shift in energy metabolism and increases the resistance of neurons to metabolic and oxidative stress. Neuromolecular Med *8*, 389-413.

Liu, D., Chan, S.L., de Souza-Pinto, N.C., Slevin, J.R., Wersto, R.P., Zhan, M., Mustafa, K., de Cabo, R., and Mattson, M.P. (2006b). Mitochondrial UCP4 mediates an adaptive shift in energy metabolism and increases the resistance of neurons to metabolic and oxidative stress. Neuromolecular Med *8*, 389-414.

Mao, W., Yu, X., Zhong, A., Li, W., Brush, J., Sherwood, S., Adams, S., and Pan, G. (1999). UCP4, a novel brain-specific mitochondrial protein that reduces membrane potential in mammalian cells. FEBS Lett *443*, 326-330.

Mark, F., Lucassen, M., and Portner, H. (2006). Thermal sensitivity of uncoupling protein expression in polar and temperate fish. Comp Biochem Physiol Part D Genomics Proteomics *1*, 365-374.

Mattiasson, G., Shamloo, M., Gido, G., Mathi, K., Tomasevic, G., Yi, S., Warden, C., Castilho, R., Melcher, T., and Gonzalez-Zulueta, M. (2003a). Uncoupling protein-2 prevents neuronal death and diminishes brain dysfunction after stroke and brain trauma. Nat Med *9*, 1062-1068.

Mattiasson, G., Shamloo, M., Gido, G., Mathi, K., Tomasevic, G., Yi, S., Warden, C.H., Castilho, R.F., Melcher, T., Gonzalez-Zulueta, M., *et al.* (2003b). Uncoupling protein-2 prevents neuronal death and diminishes brain dysfunction after stroke and brain trauma. Nat Med *9*, 1062-1068.

Mignotte, B., and Vayssiere, J. (2001). Mitochondria and apoptosis. Eur J Biochem *252*, 1-15.

Portner, H., Lucassen, M., and Storch, D. (2005). Metabolic biochemistry: its role in thermal tolerance and in the capacities of physiological and ecological function. Fish Physiol *21*, 79-154.

Prosser, C., and Nelson, D. (1981). The role of nervous systems in temperature adaptation of poikilotherms. Annu Rev Physiol *43*, 281-300.

Saito, S., Saito, C.T., and Shingai, R. (2008). Adaptive evolution of the uncoupling protein 1 gene contributed to the acquisition of novel nonshivering thermogenesis in ancestral eutherian mammals. Gene *408*, 37-44.

Shaklee, J., Christiansen, J., Sidell, B., Prosser, C., and Whitt, G. (1977). Molecular aspects of temperature acclimation in fish: Contributions of changes in enzymes patterns to metrabolic reorganization in the green sun fish. J Exp Zool *201*, 1-20.

Sies, H., Cadenas, E., Symons, M., and Scott, G. (1985). Oxidative Stress: Damage to Intact Cells and Organs [and Discussion]. Philos Trans R Soc Lond B Biol Sci *311*, 617-631.

Sohal, R.S., and Allen, R.G. (1986). Relationship between oxygen metabolism, aging and development. Adv. Free Radical Biol *2*, 117-160.

Sokolova, I.M., and Sokolov, E.P. (2005). Evolution of mitochondrial uncoupling proteins: novel invertebrate UCP homologues suggest early evolutionary divergence of the UCP family. FEBS Lett *579*, 313-317.

Stuart, J.A., Harper, J.A., Brindle, K.M., and Brand, M.D. (1999). Uncoupling protein 2 from carp and zebrafish, ectothermic vertebrates. Biochim Biophys Acta *1413*, 50-54.

Tang, S., Sun, K., Sun, G., Lin, G., Lin, W., and Chuang, M. (1999). Cold-induced ependymin expression in zebrafish and carp brain: implications for cold acclimation. FEBS Lett *459*, 95-99.

Thisse, B., Heyer, V., Lux, A., Alunni, V., Degrave, A., Seiliez, I., Kirchner, J., Parkhill, J.P., and Thisse, C. (2004). Spatial and temporal expression of the zebrafish genome by large-scale *in situ* hybridization screening. Methods Cell Biol *77*, 505-519.

Toyama, T., Nakamura, H., Harano, Y., Yamauchi, N., Morita, A., Kirishima, T., Minami, M., Itoh, Y., and Okanoue, T. (2004). PPAR [alpha] ligands activate antioxidant enzymes and suppress hepatic fibrosis in rats. Biochem Biophys Res Commun *324*, 697-704.

van den Burg, E., Peeters, R., Verhoye, M., Meek, J., Flik, G., and Van der Linden, A. (2005). Brain responses to ambient temperature fluctuations in fish: reduction of blood volume and initiation of a whole-body stress response. J Neurophysiol 93, 2849.

van den Burg, E.H., Verhoye, M., Peeters, R.R., Meek, J., Flik, G., and Van der Linden, A. (2006). Activation of a sensorimotor pathway in response to a water temperature drop in a teleost fish. J Exp Biol 209, 2015-2024.

Vidal-Puig, A., Solanes, G., Grujic, D., Flier, J., and Lowell, B. (1997). UCP3: an uncoupling protein homologue expressed preferentially and abundantly in skeletal muscle and brown adipose tissue. Biochem Biophys Res Commun *235*, 79-82.

Villarroya, F., Iglesias, R., and Giralt, M. (2007). PPARs in the control of uncoupling proteins gene expression. PPAR Res *2007*.

Votyakova, T.V., and Reynolds, I.J. (2001). DeltaPsi(m)-Dependent and -independent production of reactive oxygen species by rat brain mitochondria. J Neurochem *79*, 266-277.

Wang, P., Liu, J., Li, Y., Wu, S., Luo, J., Yang, H., Subbiah, R., Chatham, J., Zhelyabovska, O., and Yang, Q. (2010). Peroxisome Proliferator-Activated

Receptor[delta] Is an Essential Transcriptional Regulator for Mitochondrial Protection and Biogenesis in Adult Heart. Circ Res.

Wullimann, M.F. (1997). The Central Nervous System. *The Physiology of Fishes Second Edition*, Evans, DH, Ed, New York: Boca Raton CRS, pp. 245-282.

Yoo, H., Chang, M., and Rho, H. (1999). Induction of the rat Cu/Zn superoxide dismutase gene through the peroxisome proliferator-responsive element by arachidonic acid. Gene *234*, 87-91.

Zhang, X., Li, L., Prabhakaran, K., Zhang, L., Leavesley, H.B., Borowitz, J.L., and Isom, G.E. (2007). Uncoupling protein-2 up-regulation and enhanced cyanide toxicity are mediated by PPAR[alpha] activation and oxidative stress. Toxicol Appl Pharmacol *223*, 10-19.

Zigmond, R., Schon, F., and Iversen, L. (1974). Increased tyrosine hydroxylase activity in the locus coeruleus of rat brain stem after reserpine treatment and cold stress. Brain Res *70*, 547.

Table 1. Primers used for qRT-PCR and *in situ* probe construction

qRT-PCR primer name	**Primer sequence**	**Product size (bp)**
QzUCP1	F 5'-ACACAAACGGACTCAGACGA-3' R 5'-TGCTACGCTGAACTCATCAA-3'	112
QzUCP2	F 5'-CTAAACCGGTTAGGGTGGAG-3' R 5'-TTACAGTTGCAGCCGAAATC-3'	104
QzUCP2l	F 5'-CGCCTTTCTGAACACACAACATC-3' R 5'-TGACCTTTGGCCTTACAACACTG-3'	150
QzUCP4	F 5'-CAGCCTCGGGATTCAAAC-3' R 5'-AAGACCAGGGAGCCATTCTA-3'	139
QzPPARαa	F 5'-ATTATGTACAGCCCTCTGAGCGGA-3' R 5'-TGAGAACACTTCTGAGGACGGACT-3'	195
QzPPARαb	F 5'-GTAGACATGGAGAATCGCTACCGT-3' R 5'-AAGCTGCTGAGAGCGTCTTCAT-3'	134
QzPPARδa	F 5'-AATGCCAGTTCTGCCGCTTTCAGA-3' R 5'-TTCAGGTAGGCGTTGTTGACCCGTTT-3'	193
QzPPARδb	F 5'-AATGCCAGTACTGCCGCTTTCAGA-3' R 5'-TGTTGACGTGCTTGGCCAGTGTTT-3'	177
QzPPARγ	F 5'-TCCACAGTTTGCAGAGAACAGCGT-3' R 5'-TTGGCACTTGTTGCGGCTCTTCTT-3'	235
QzCAT	F 5'-TAAAGGAGCAGGAGCGTTTGGCTA-3' R 5'-TTCACTGCGAAACCACGAGGATCT-3'	177
QzUCP5	F 5'-ACTCCTGGCAGCTACCGTAT-3' R 5'-CTCAAGCCAGTGTGGAGAAA-3'	165
QzRPL13a	F 5'-CCTCGGTCGTCTTTCCGCTATTG-3' R 5'-CAGCCTGACCCCTCTTGGTTTTG-3'	248
***in situ* probe primer name**	**Primer sequence**	**Product size (bp)**
zUCP1_IS	F 5'-CAACTGCACAGAACTGGTGTCTTACGATCT-3' R 5'-ATAGCCATACACCCAAAGCACTTCACAAT-3'	1201
zUCP2_IS	F 5'-GCACGAGTTCTCAACGTTTCTCTATGGAAGA-3' R 5'-TGGCCCGTTTCAGCTGCTCGTAAGT-3'	1110
zUCP2l_IS	F 5'-GCAAGTGTTGTGCTGCTGTTATGCTGCTTT-3' R 5'-GGGATTCCTCCATTCTCACAACAGAGCGTT-3'	1208
zUCP4_IS	F 5'-TTCAGGCTCGTGGTTCCTTTGGGACATAGT-3' R 5'-AAAGACCAGGGAGCCATTCTAAACCACGTTG-3'	976
zUCP5_IS	F 5'-ACGAGAGGAAGGCGTCCGGGCATTGT-3' R 5'-GGAGTCTGCCGACCTCAAATATTCCTCAGGG-3'	1200

F, forward primer; R, reverse primer

Table 2. Identities (in percent) of amino acid sequences among the identified zebrafish UCP (zUCP) isoforms

Identity (%)	***zucp1***	***zucp2***	***zucp2l***	***zucp4***	***zucp5***
zucp1	—	72	46	33	33
zucp2		—	50	32	34
zucp2l			—	23	22
zucp4				—	36
zucp5					—

Table 3. Summary of the detailed *zucps* mRNA expression patterns in zebrafish brain

	zucp1	***zucp2***	***zucp2l***	***zucp4***	***zucp5***
Telencephalon	-	Vl	-	?	?
Diencephalon					
- Epithalamus	-	Ha	-	-	-
- Dorsal thalamus	-	DP	CP	-	-
- Ventral thalamus	VM	VM	VM	VM	VM
- Posterior tuberculum	-	-	-	TPp	-
Mescencephalon					
- tectum opticum	PGZ	PGZ, TL	PGZ	PGZ	PGZ
Cerebellum					
- Vestibulolateralis lobe	-	EG, LCa	-	EG, LCa	EG, LCa
- Corpus cerebelli	-	CCe	-	CCe	CCe
- Valvula cerebelli	Vam	Val	Vam	Val	-
Medulla oblongata	CC	CC	CC	CC	?

CC, cerebellar crest; CCe, cerebellar corpus; CP, central posterior thalamic nucleus; DP, dorsal posterior thalamic nucleus; EG, granular eminence; Ha, habenula; LCa, caudal lobe of cerebellum; PGZ, periventricular gray zone of optic tectum; TL, longitudinal torus; TPp, periventricular nucleus of posterior tuberculum; Val, lateral division of valvula cerebelli; Vam, valvula crebelli; Vl, lateral nucleus of ventral telecephalic area; VM, ventromedial thalamic nucleus.

Table 4. List of species and accession numbers for UCP sequences

Species name	**Protein name**	**Accession number**
Homo sapiens	Human UCP1	NP_068605
Mus musculus	Mouse UCP1	NP_033489
Ornithorhynchus anatinus	Platypus UCP1	XP_001512700
Xenopus tropicalis	Frog UCP1	NP_001107354
Cyprinus carpio	Carp UCP1	AAS10175
Fugu rubripes	Pufferfish UCP1	ENSTRUP00000033443*
Danio rerio	Zebrafish UCP1	NP_955817
Ciona intestinalis	Sea squirt UCPX	XP_002129757
Homo sapiens	Human UCP2	NP_003346
Mus musculus	Mouse UCP2	NP_035801
Monodelphis domestica	Opossum UCP2	XP_001362966
Xenopus tropicalis	Frog UCP2	NP_989179
Oncorhynchus mykiss	Trout UCP2A	ABC00183
Oncorhynchus mykiss	Trout UCP2B	ABC00185
Cyprinus carpio	Carp UCP2	CAB46248
Tetraodon nigroviridis	Tetraodon UCP2	GSTENP00022194001*
Tetraodon nigroviridis	Tetraodon UCP2-like	GSTENT00022195001*
Fugu rubripes	Pufferfish UCP2	ENSTRUP00000037074*
Fugu rubripes	Pufferfish UCP2-like	ENSTRUP00000037001*
Danio rerio	Zebrafish UCP2	NP_571251
Danio rerio	Zebrafish UCP2-like	NP_956647
Homo sapiens	Human UCP3-similar (short variant)	NP_073714
Homo sapiens	Human UCP3-like (long variant)	NP_003347
Mus musculus	Mouse UCP3	NP_033490
Monodelphis domestica	Opossum UCP3	XP_001368096
Ornithorhynchus anatinus	Platypus UCP3	XP_001512822
Gallus gallus	Chicken UCP3	NP_989438
Homo sapiens	Human UCP4	NP_004268
Mus musculus	Mouse UCP4	NP_082987
Monodelphis domestica	Opossum UCP4	XP_001368742
Xenopus tropicalis	Frog UCP4	ENSXETP00000035487*
Danio rerio	Zebrafish UCP4	NP_956635

Ciona intestinalis	Sea squirt UCP4	XP_002125994
Homo sapiens	Human UCP5	NP_003942
Mus musculus	Mouse UCP5	NP_035528
Monodelphis domestica	Opossum UCP5	XP_001381468
Gallus gallus	ChickenUCP5	NP_001012901
Fugu rubripes	Pufferfish UCP5	ENSTRUP00000023155*
Danio rerio	Zebrafish UCP5	NP_956458

* Sequences obtained form the Ensembl database.

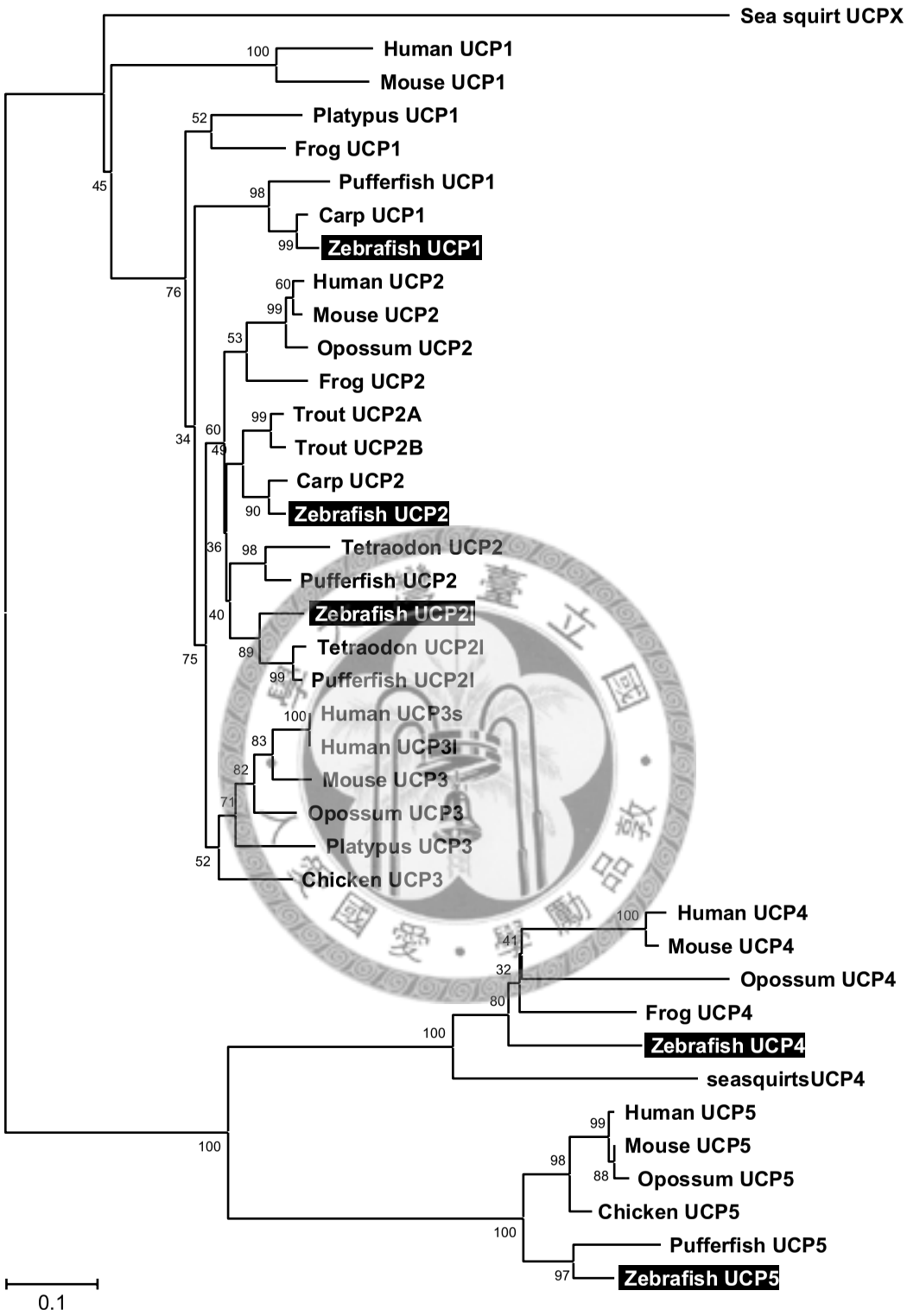

Figure 1. Phylogenetic analysis of UCP amino acid sequences. The putative sequences of other species were obtained from the NCBI and Ensembl databases.Consensus trees were generated using the Neighbor-joining method with the pairwise deletion gap calculating option. The results were confirmed by 1000 bootstraps. The unit of scale bar is the number of amino acid substitutions per site.

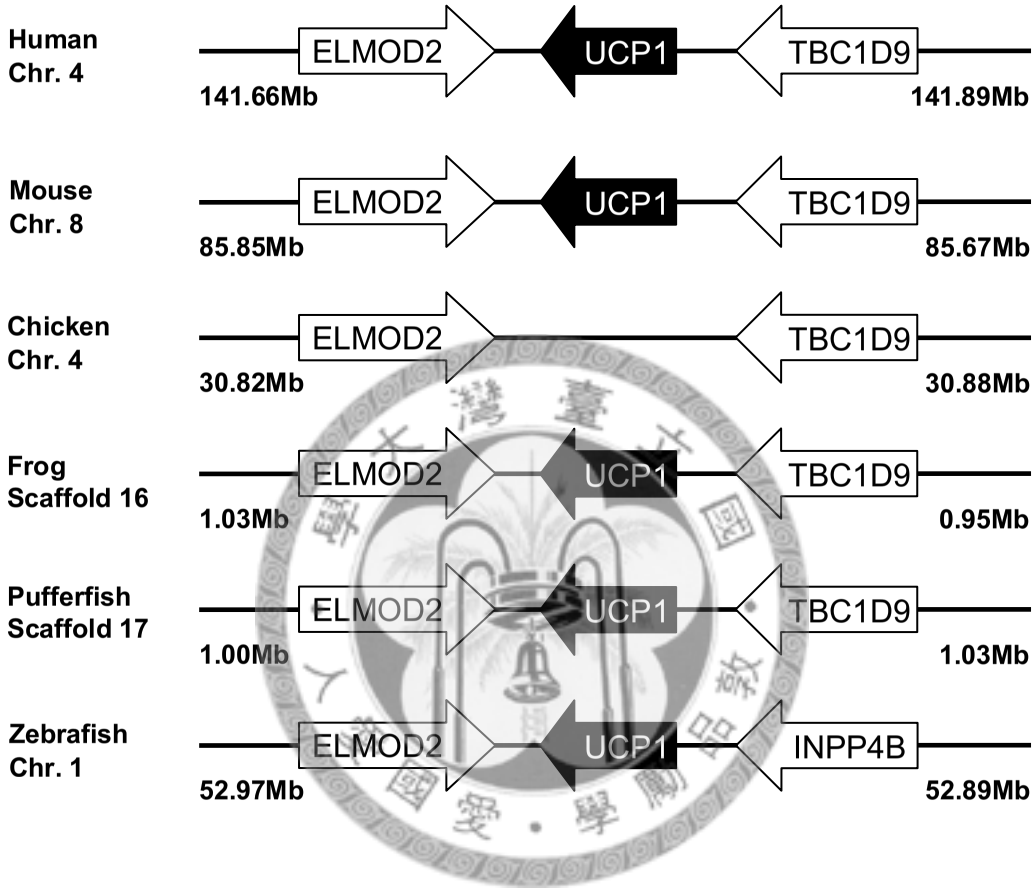

Figure 2. Gene structures encompassing UCP1 orthologues. The physical distance of the genomic region is indicated on both sides. Chr., the chromosome. The arrow indicates the gene with the direction. All sequences of UCP orthologs obtained from the NCBI and Ensembl database are referring to Table 4. Those *zucp* neighboring transcripts were identified utilizing the Ensembl genome browser system. ELMOD2, ELMO/CED-12 domain containing 2; INPP4B, inositol polyphosphate-4-phosphatase, type II; TBC1D9, TBC1 domain family, member 9.

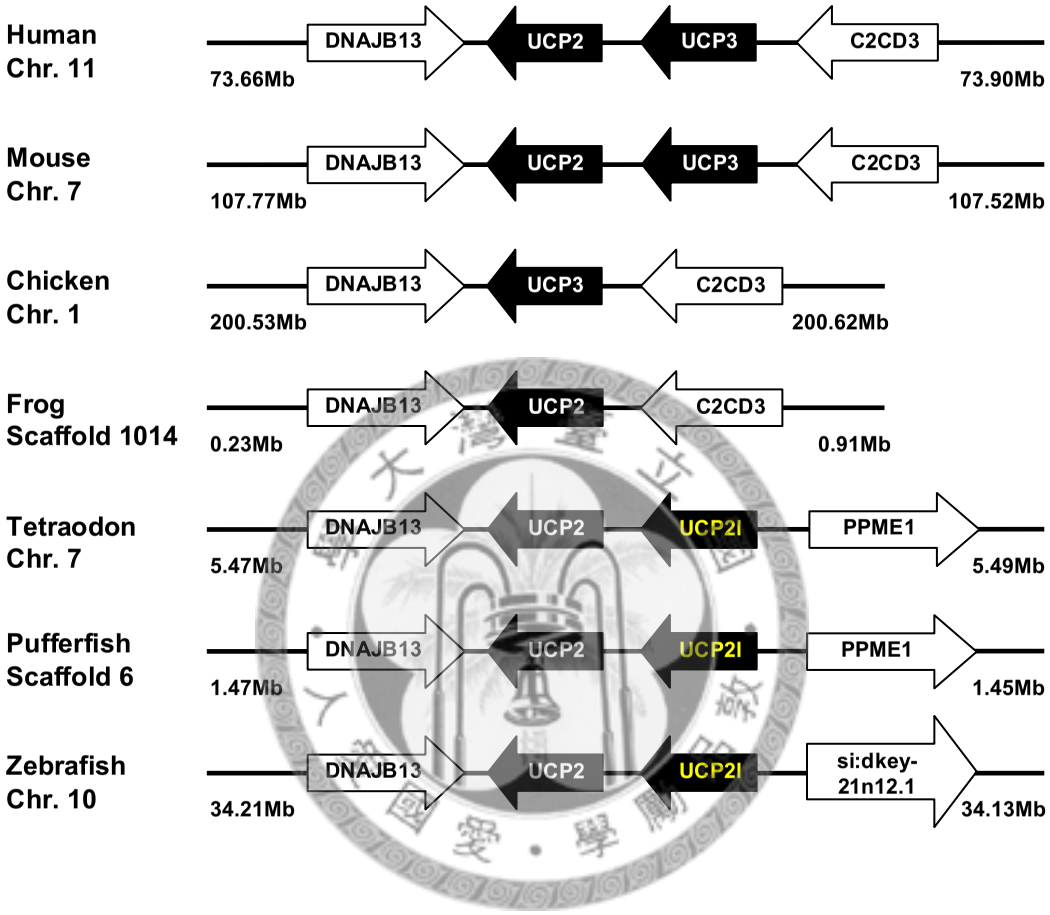

Figure 3. Gene structures encompassing UCP2 orthologues. The physical distance of the genomic region is indicated on both sides. Chr., the chromosome. The arrow indicates the gene with the direction. All sequences of UCP orthologs obtained from the NCBI and Ensembl database are referring to Table 4. Those *zucp* neighboring transcripts were identified utilizing the Ensembl genome browser system. C2CD3, C2 calcium-dependent domain containing 3; DNAJB13, DnaJ (Hsp40) homolog, subfamily B, member 13; PPME1, protein phosphatase methylesterase 1; si:dkey-21n12.1, si:dkey-21n12.1 protein.

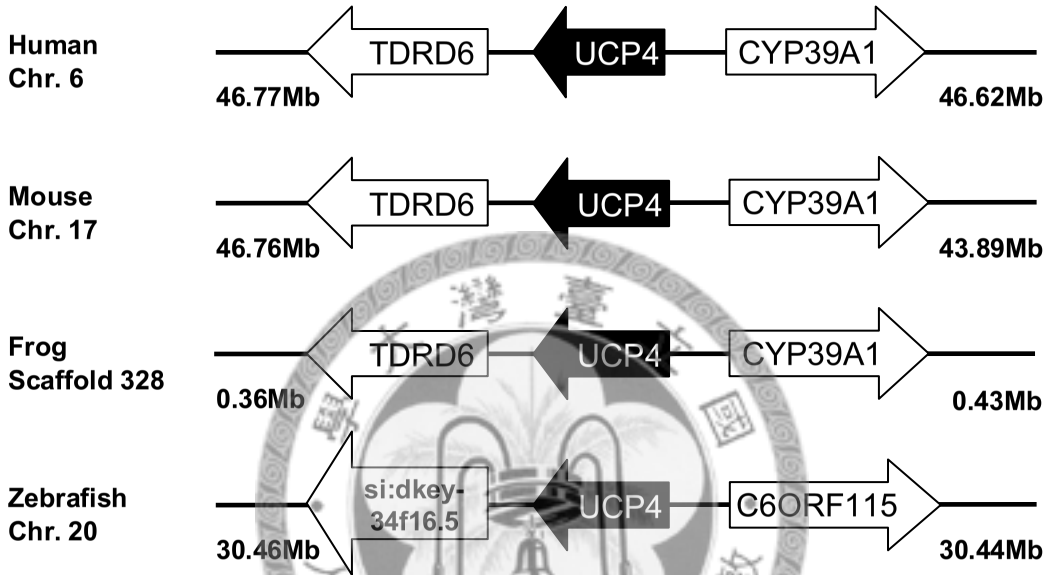

Figure 4. Gene structures encompassing UCP4 orthologues. The physical distance of the genomic region is indicated on both sides. Chr., the chromosome. The arrow indicates the gene with the direction. All sequences of UCP orthologs obtained from the NCBI and Ensembl database are referring to Table 4. Those *zucp* neighboring transcripts were identified utilizing the Ensembl genome browser system. C6orf115, chromosome 6 open reading frame 115; CYP39A1, cytochrome P450, family 39, subfamily A, polypeptide 1; si:dkey-34f16.5, si:dkey-34f16.5 protein; TDRD6, tudor domain containing 6.

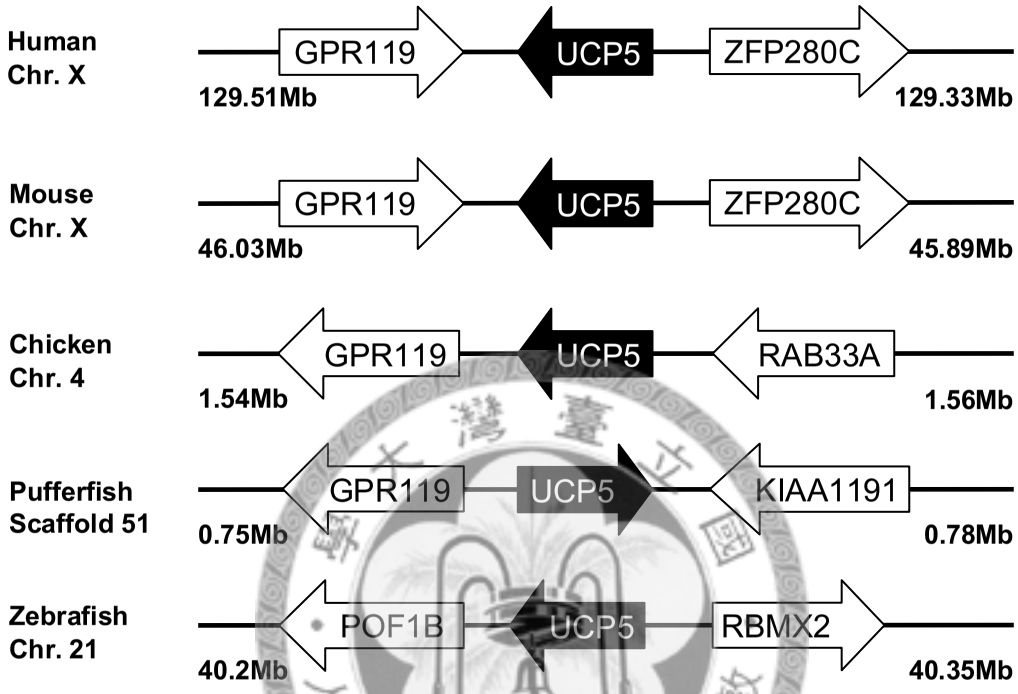

Figure 5. Gene structures encompassing UCP5 orthologues. The physical distance of the genomic region is indicated on both sides. Chr., the chromosome. The arrow indicates the gene with the direction. All sequences of UCP orthologs obtained from the NCBI and Ensembl database are referring to Table 4. Those *zucp* neighboring transcripts were identified utilizing the Ensembl genome browser system. GPR119, G protein-coupled receptor 119; KIAA1191, KIAA1191 protein; POF1B, premature ovarian failure, 1B; RAB33A, RAB33A, member RAS oncogene family; RBMX2, RNA binding motif protein, X-linked 2; ZFP280C, zinc finger protein 280C.

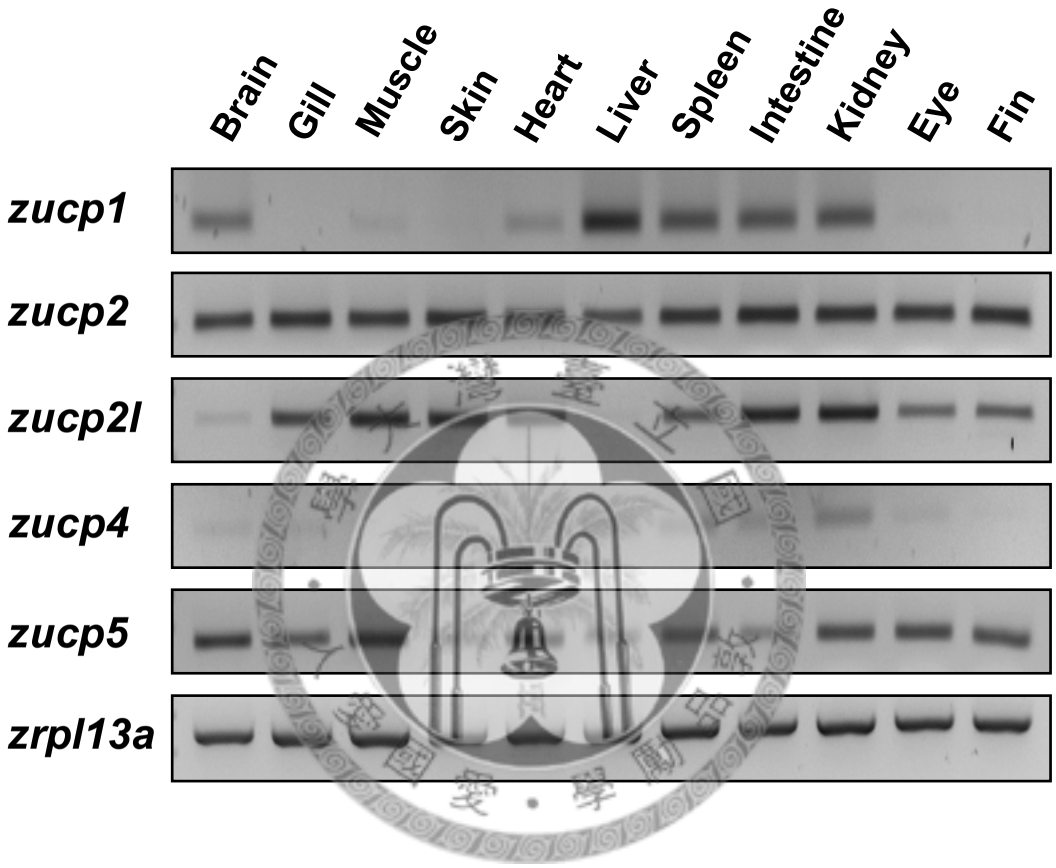

Figure 6. RT-PCR analysis of *zucp* mRNA expressions in various tissues of zebrafish with isoform-specific primer sets. *rpl13a* was used as the internal control.

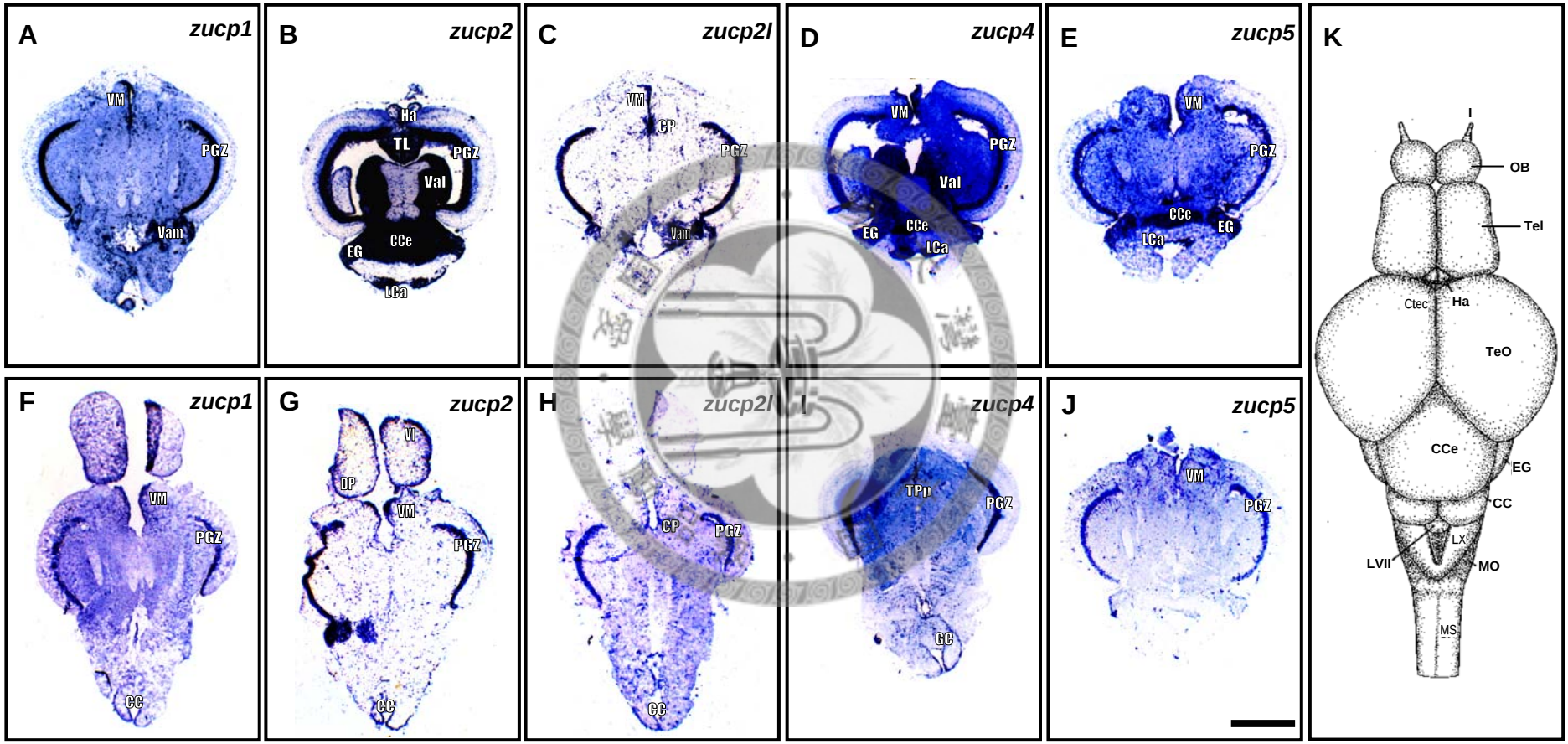
A
zucp1
VM
PGZ
Vam
B
zucp2
Ha
TL
PGZ
Val
CCe
EG
LCa
C
zucp2l
VM
CP
PGZ
Vam
D
zucp4
VM
PGZ
Val
EG
CCe
LCa
E
zucp5
VM
PGZ
CCe
EG
LCa
K
I
OB
Tel
Ctec
Ha
TeO
CCe
EG
CC
LX
LVII
MO
MS
F
zucp1
VM
PGZ
GC
G
zucp2
Vl
DP
VM
PGZ
GC
H
zucp2l
CP
PGZ
GC
I
zucp4
TPp
PGZ
GC
J
zucp5
VM
PGZ

Figure 7. mRNA in situ hybridization of *zucp* paralogues in brains' crosssection of adult zebrafish. All the five *zucps* were observed in diencephalon, mescencephalon, and cerebellum. In addition, except the *zucp5, zucp1, -2, -2l, -4* were all expressed in medulla oblongata. Besides, *zucp2* mRNA also distributed in telencephalon. Detailed mRNA expression patterns of *zucps* in zebrafish brain were listed in Table. 2. CC, cerebellar crest; CCe, cerebellar corpus; CP, central posterior thalamic nucleus; Ctec, commissura tecti; DP, dorsal posterior thalamic nucleus; EG, granular eminence; Ha, habenula; I, olfactory nerve ; LCa, caudal lobe of cerebellum; LVII, facial lobe; LX, vegal lobe; MO, medulla oblongata; MS, medulla spinalis; OB, olfactory bulb; PGZ, periventricular gray zone of optic tectum; Tel, telencephalon; TeO, tectum opticum; TL, longitudinal torus; TPp, periventricular nucleus of posterior tuberculum; Val, lateral division of valvula cerebelli; Vam, valvula crebelli; Vl, lateral nucleus of ventral telecephalic area; VM, ventromedial thalamic nucleus. Scale bar: 600 μm.

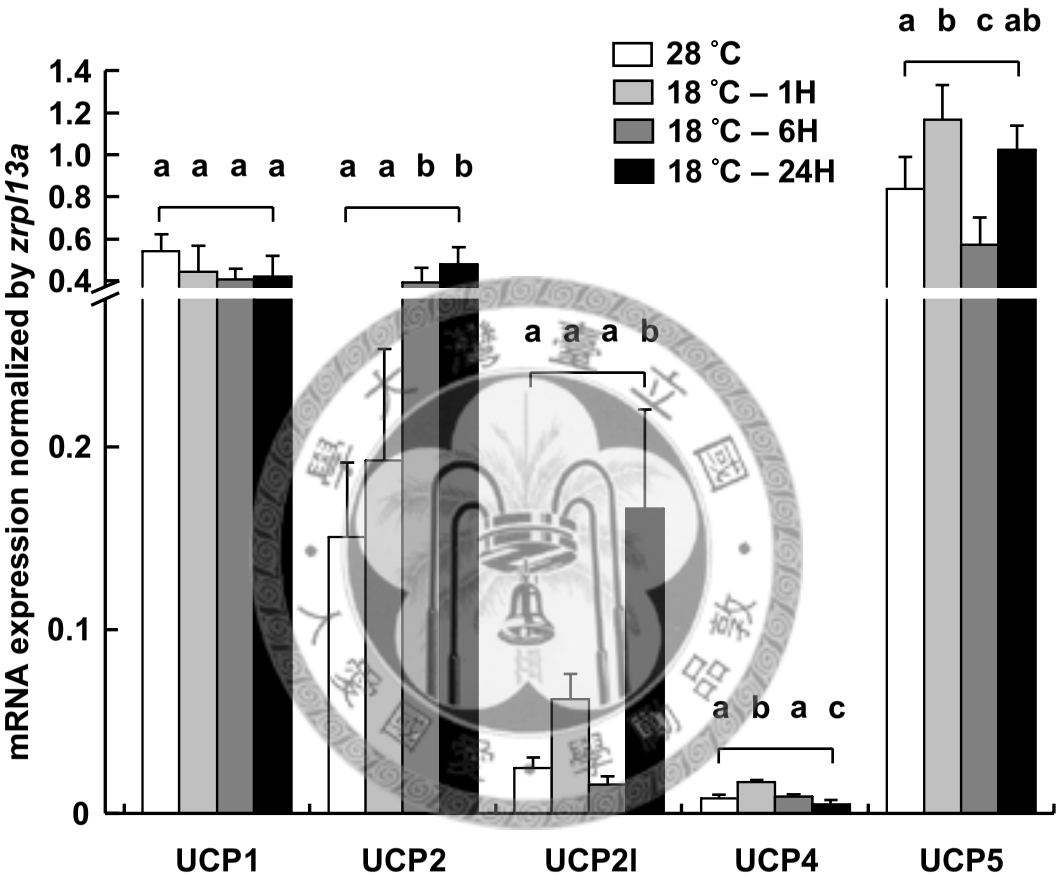

Figure 8. qPCR analysis of the mRNA expressions of 5 *zucp* isoforms in brains of zebrafish at 28 ˚C and 1-, 6-, 24- hour after transfer to 18 ˚C. *rpl13a* was used as the internal control. Data are presented as mean ± SD (N=4). Different letters indicate significant differences between treatments (one-way ANOVA, Tukey's pairwise comparison, $p<0.05$).

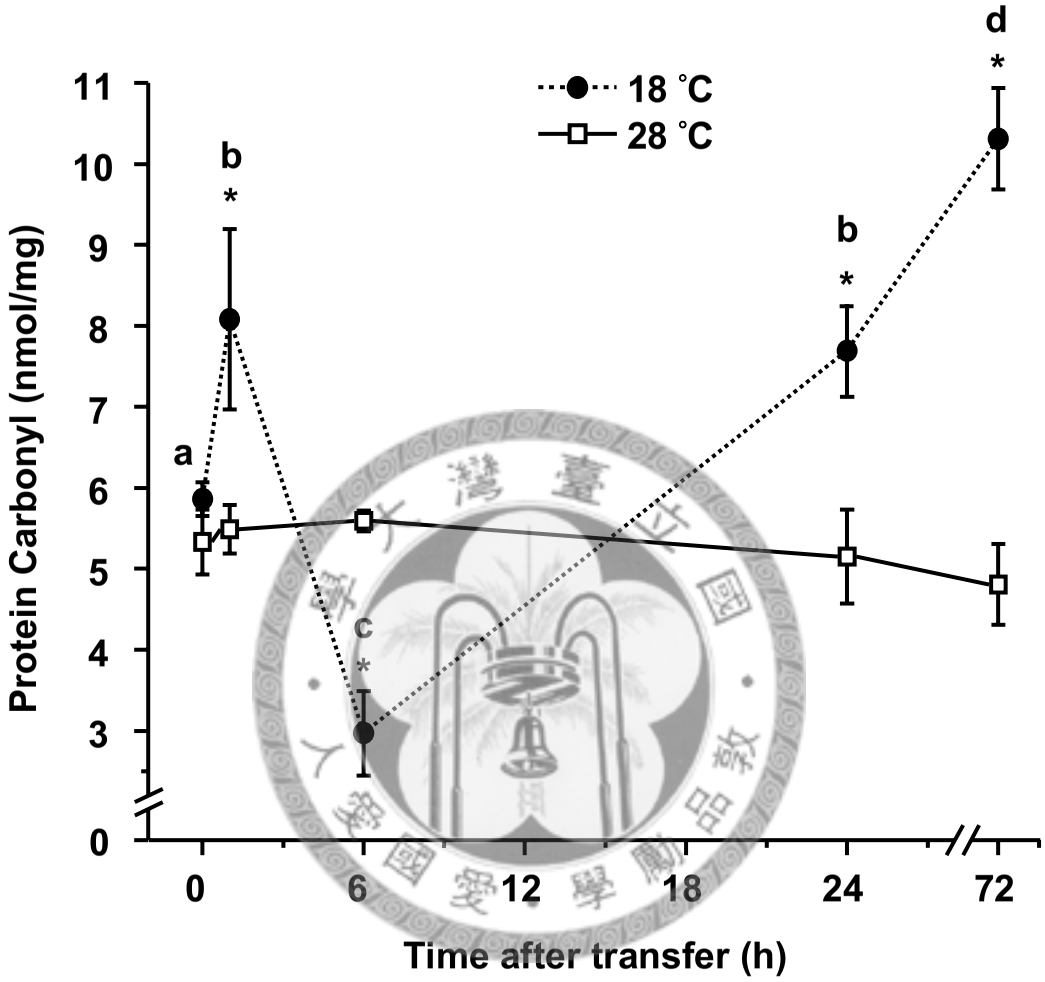

Figure 9. Time-course changes in zebrafish brains' protein carbonyl contents transferred from 28 ˚C (0 h) to 18 ˚C. The carbonyl contents were measured by detecting the dinitrophenylhydrazone (DNP). The solid line represents the 28 ˚C control group, and the dashed line represents the 18 ˚C treatment group. Data are presented as means ± SD. (*N*=6). *Indicates a significant difference from the respective control in 28 ˚C (p<0.05). Different letters indicate significant differences (p<0.05) among sampling times in fish transferred to 18˚C.

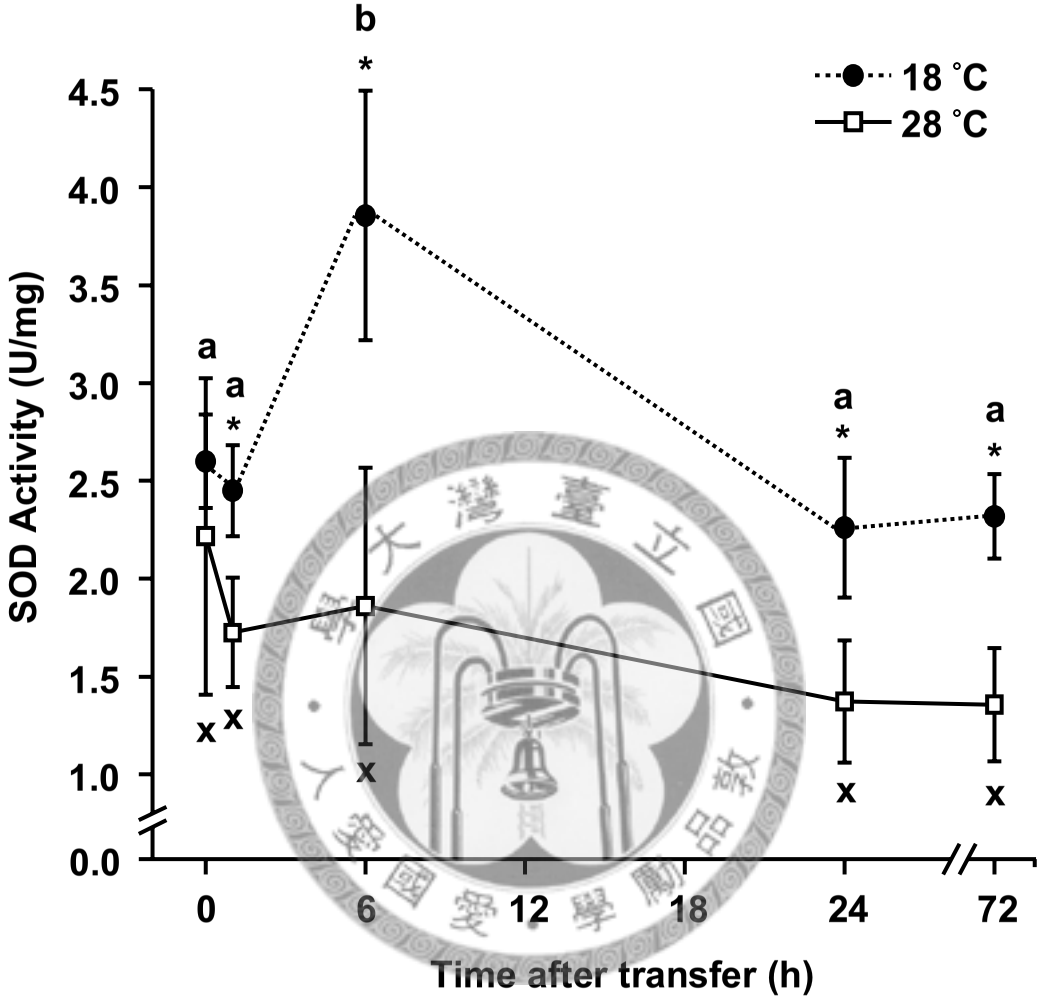

Figure 10. Time-course changes in zebrafish brains' superoxide dismutase (SOD) activities transferred from 28 ˚C (0 h) to 18 ˚C. The SOD activities were determined with xanthine/xanthine oxidase (XOD) system. The solid line represents the 28 ˚C control group, and the dashed line represents the 18 ˚C treatment group. Data are presented as means± SD. (*N*=6). *Indicates a significant difference from the respective control in 28 ˚C ($p<0.05$). Different letters indicate significant differences ($p<0.05$) among sampling times in fish transferred to 18 ˚C.

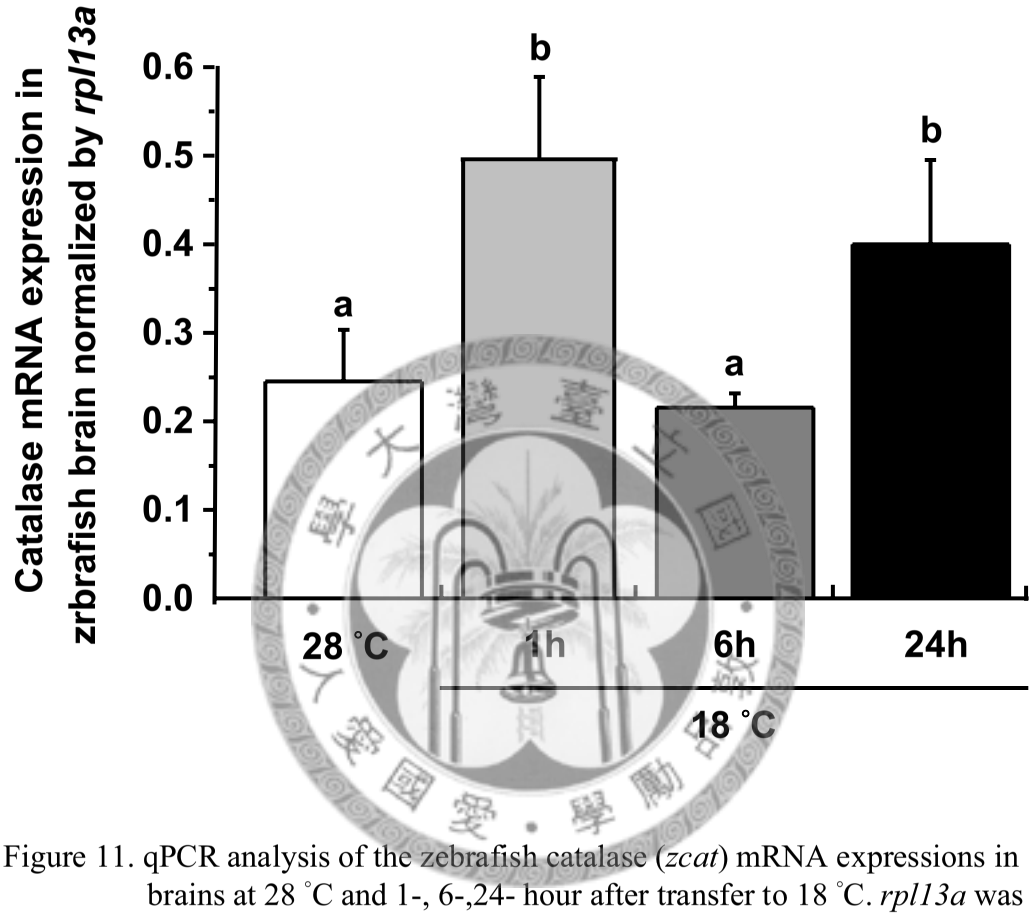

Figure 11. qPCR analysis of the zebrafish catalase (*zcat*) mRNA expressions in brains at 28 ˚C and 1-, 6-,24- hour after transfer to 18 ˚C. *rpl13a* was used as the internal control. Data are presented as mean ± SD (*N*=4). Different letters indicate significant differences between treatments (one-way ANOVA, Tukey's pairwise comparison, $p<0.05$).

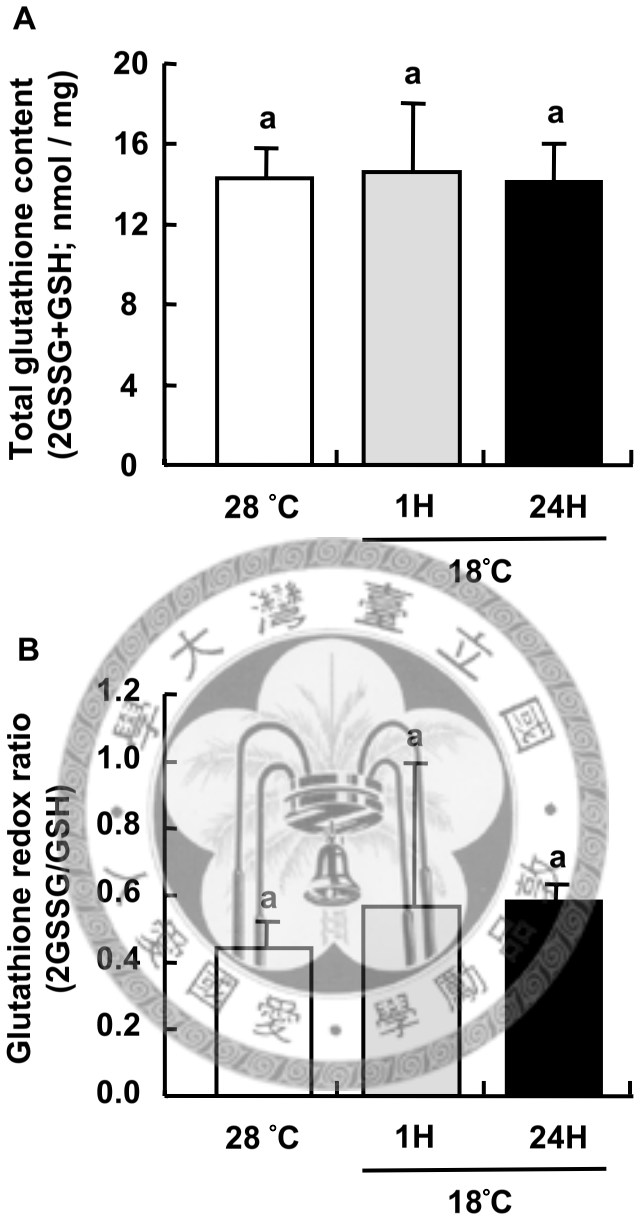

Figure 12. Glutathione redox chemistry in zebrafish brains at 28 ˚C and 1-, 24-hour after transfer to 18 ˚C. (A) total glutathione content (2GSSG+GSH); (B) glutathione redox ratio (2GSSG/GSH). Data are presented as mean ± SD (*N*=4). Different letters indicate significant differences between treatments (one-way ANOVA, Tukey's pairwise comparison, $p<0.05$).

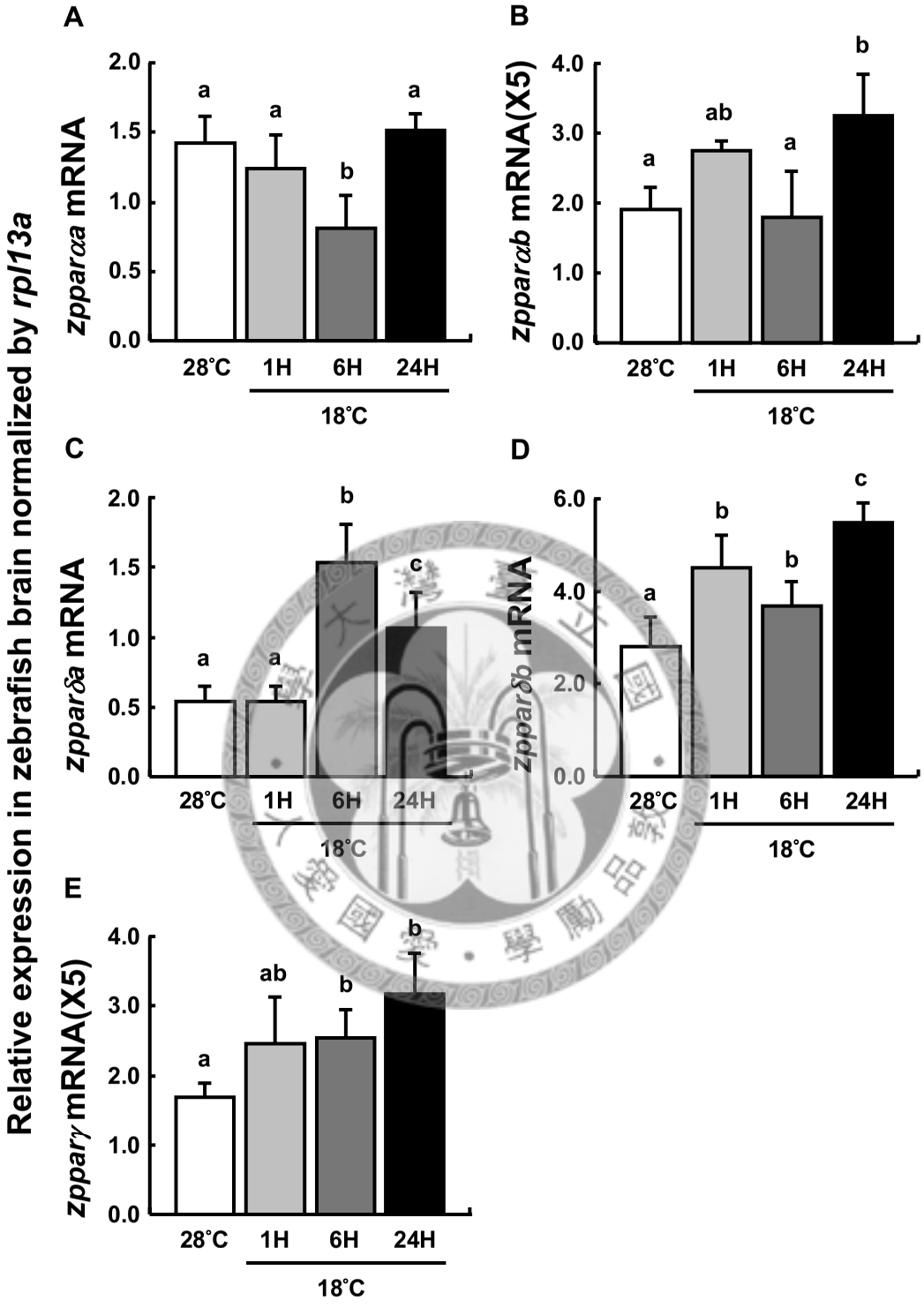

Figure 13. qPCR analysis of different types and isoforms of *zppar* mRNA expressions in zebrafish brains at 28 ˚C and 1-, 6-, 24- hour after transfer to 18 ˚C. (A) *zpparαa* mRNA (B) *zpparαb* mRNA (C) *zpparδa* mRNA (D) *zpparδb* mRNA (E) *zpparγ* mRNA. *rpl13a* was used as the internal control. Data are presented as mean ± SD (*N*=4). Different letters indicate significant differences between treatments (one-way ANOVA, Tukey's pairwise comparison, $p<0.05$).

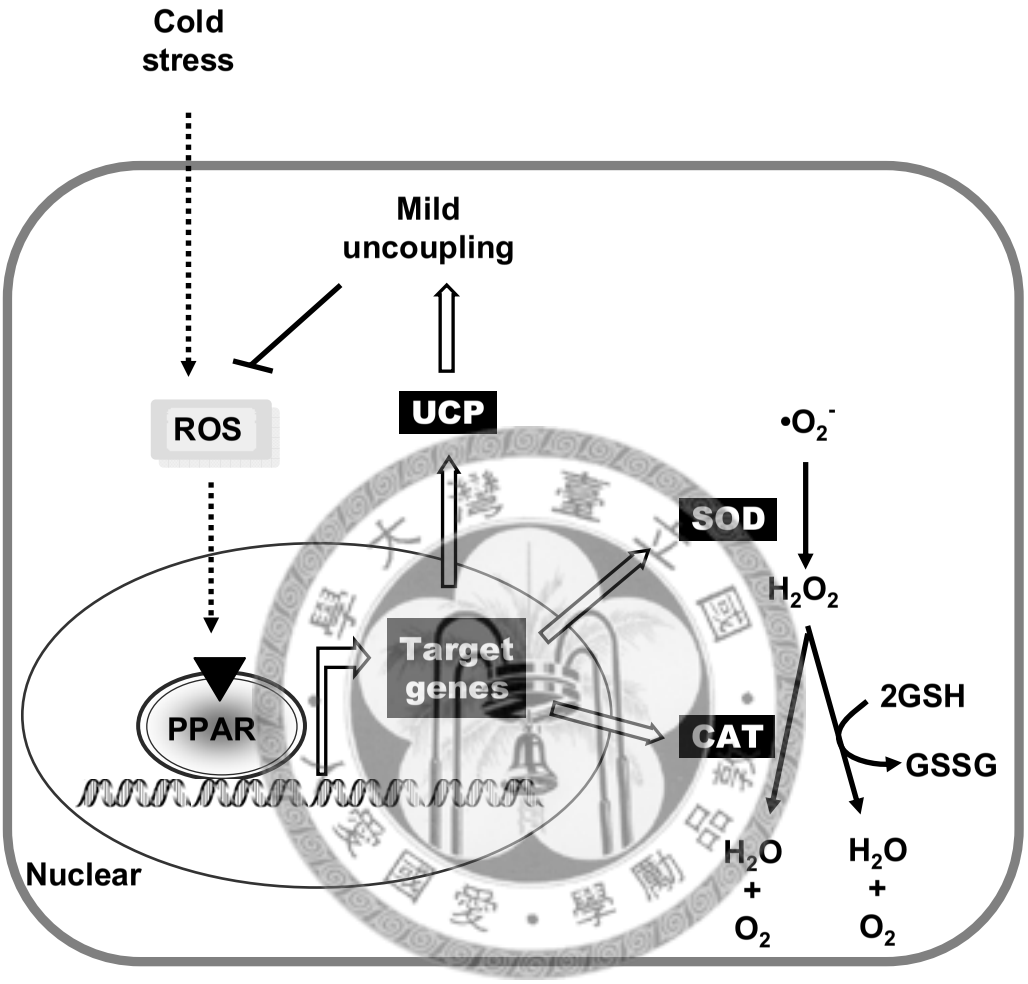

Figure 14. Schematic diagram illustrating physiological pathways postulated for cold-induced oxidative stress in zebrafish brain and antioxidantal effects of PPARs. Acute cold exposure increases ROS levels in zebrafish brain, which activate the PPARs. Activated PPARs may enhance the expression of their target genes, including UCPs, SOD and CAT. Increased SOD activity and *cat* expression reduce the superoxide into H_2O and O_2 , thus eliminate the ROS accumulation. In addition, activated UCPs may reduce the mitochondrial ROS levels through mild uncoupling. Open and filled arrows indicate causal relationships postulated in the present study, and dotted arrows indicate indirect causal relationships.